batteries

MDPI

Review

MXenes in Solid-State Batteries: Multifunctional Roles from Electrodes to Electrolytes and Interfacial Engineering

Francisco Márquez

Nanomaterials Research Group, Department of Natural Sciences and Technology, Division of Natural Sciences, Technology and Environment, Universidad Ana G. Méndez-Gurabo Campus, Gurabo, PR 00778, USA; fmarquez@uagm.edu; Tel.: +1-787-743-7979 (ext. 4250)

Abstract

MXenes, a rapidly emerging family of two-dimensional transition metal carbides and nitrides, have attracted considerable attention in recent years for their potential in next-generation energy storage technologies. In solid-state batteries (SSBs), they combine metallic-level conductivity (>10^3 S cm^{-1}), adjustable surface terminations, and mechanical resilience, which makes them suitable for diverse functions within the cell architecture. Current studies have shown that MXene-based anodes can deliver reversible lithium storage with Coulombic efficiencies approaching ~98% over 500 cycles, while their use as conductive additives in cathodes significantly improves electron transport and rate capability. As interfacial layers or structural scaffolds, MXenes effectively buffer volume fluctuations and suppress lithium dendrite growth, contributing to extended cycle life. In solid polymer and composite electrolytes, MXene fillers have been reported to increase Li^+ conductivity to the 10^{-3}–10^{-2} S cm^{-1} range and enhance Li^+ transference numbers (up to ~0.76), thereby improving both ionic transport and mechanical stability. Beyond established Ti-based systems, double transition metal MXenes (e.g., Mo_2TiC_2, $Mo_2Ti_2C_3$) and hybrid heterostructures offer expanded opportunities for tailoring interfacial chemistry and optimizing energy density. Despite these advances, large-scale deployment remains constrained by high synthesis costs (often exceeding USD 200–400 kg^{-1} for $Ti_3C_2T_x$ at lab scale), restacking effects, and stability concerns, highlighting the need for greener etching processes, robust quality control, and integration with existing gigafactory production lines. Addressing these challenges will be crucial for enabling MXene-based SSBs to transition from laboratory prototypes to commercially viable, safe, and high-performance energy storage systems. Beyond summarizing performance, this review elucidates the mechanistic roles of MXenes in SSBs—linking lithiophilicity, field homogenization, and interphase formation to dendrite suppression at Li | SSE interfaces, and termination-assisted salt dissociation, segmental-motion facilitation, and MWS polarization to enhanced electrolyte conductivity—thereby providing a clear design rationale for practical implementation.

Keywords: MXene; all-solid-state batteries (ASSBs); energy storage; interfacial engineering; lithium metal anode; solid electrolyte

Academic Editor: Pascal Venet

Received: 29 August 2025
Revised: 28 September 2025
Accepted: 29 September 2025
Published: 2 October 2025

Citation: Márquez, F. MXenes in Solid-State Batteries: Multifunctional Roles from Electrodes to Electrolytes and Interfacial Engineering. *Batteries* **2025**, *11*, 364. https://doi.org/10.3390/batteries11100364

1. Introduction

Solid-state batteries (SSBs) are widely regarded as one of the most promising next-generation energy storage technologies, driven by the urgent need for safer, higher-energy-density, and longer-lasting solutions for electric vehicles (EVs), portable electronics, and grid-scale applications. The rapid growth of electrified transportation and renewable

integration imposes stringent demands on battery systems, including high energy density, fast charging, long cycle life, and reliable safety under harsh operating conditions.

Conventional lithium-ion batteries (LIBs), despite dominating the market for nearly three decades, rely on flammable liquid electrolytes that introduce risks such as leakage, volatility, and thermal runaway under mechanical stress or overcharge scenarios [1,2]. These inherent limitations have stimulated worldwide efforts to replace liquid electrolytes with solid-state electrolytes (SSEs), which offer enhanced safety and improved performance. By enabling the use of lithium metal as the anode, providing a theoretical specific capacity of 3860 mAh g^{-1} and the lowest electrochemical potential (−3.04 V vs. SHE)—SSEs can potentially double the energy density of state-of-the-art LIBs [3,4]. In addition, their superior mechanical properties help mitigate lithium dendrite formation, a major failure mode in liquid-based cells, while their broad electrochemical stability window supports the integration of high-voltage cathode materials [5,6]. Nevertheless, the practical deployment of SSBs is still hindered by a set of coupled bottlenecks that go beyond general safety arguments, namely moderate room-temperature ionic conductivities in many oxides (~10^{-4}–10^{-3} S cm^{-1}) and moisture sensitivity in fast-conducting sulfides that can release H_2S [7–9], high and evolving interfacial resistance at Li metal/SSE due to poor wetting, void formation during stripping, and dendrite penetration along defects even in dense ceramics [2,10], electrochemical incompatibility leading to interphase growth that consumes active Li/electrolyte at both anode and cathode sides [11], contact loss and mechanical mismatch in rigid stacks that require sustained pressure, transport limitations in thick composite cathodes that simultaneously need robust electronic percolation and facile Li^+ pathways, and manufacturing constraints related to brittleness/processing of oxides and moisture sensitivity of sulfides. Addressing these specific hurdles—ionic transport, interfacial stability, chemical compatibility, mechanical integrity, cathode architecture, and manufacturability—is central to translating SSBs from laboratory demonstrations to practical devices. Overcoming these challenges requires innovative materials that combine high ionic conductivity, chemical and electrochemical stability, mechanical robustness, and interfacial compatibility. Recent advances in materials chemistry have introduced two-dimensional (2D) materials as promising candidates to address these issues. Among them, MXenes, a family of 2D transition metal carbides, nitrides, and carbonitrides, have attracted considerable attention due to their unique combination of properties. First discovered by Gogotsi and Barsoum in 2011 through selective etching of the A-layer (typically Al) from MAX phases, MXenes possess the general formula $M_{n+1}X_nT_x$, where M represents an early transition metal, X is carbon and/or nitrogen, and Tx denotes surface terminations [12,13]. The structural diversity, tunable surface chemistry, and high electronic conductivity of MXenes make them ideal for electrochemical applications [14]. Details of synthesis routes and etching approaches are provided in Section 2.2. Crucially for SSBs, MXenes couple metallic-level conductivity with hydrophilic, termination-rich surfaces and mechanically compliant, processable sheets—features that are exceptionally well suited for engineering interfaces and transport in all-solid architectures.

MXenes exhibit hydrophilic surfaces and flexible layered structures with tunable interlayer spacing, enabling efficient ion transport and intercalation. Their excellent electronic conductivity facilitates fast charge transfer, which is crucial for battery electrodes and interfacial layers [15]. Furthermore, their mechanical flexibility and processability allow the fabrication of dense films and coatings, overcoming limitations of brittle ceramic materials. In energy storage, MXenes have demonstrated exceptional performance as supercapacitor electrodes due to their high volumetric capacitance [16], as lithium-ion battery anodes with high rate capability and cycling stability [17], and more recently as sodium-ion and potassium-ion battery electrodes [18]. Their unique ability to combine

surface redox (pseudocapacitance) and intercalation mechanisms enables fast kinetics and high power densities, characteristics desirable for advanced batteries [19]. In the specific context of SSBs, and to move beyond generic statements, we explicitly connect MXene functionalities to the concrete bottlenecks identified above: (i) as ultrathin, lithiophilic and highly conductive interlayers at the Li/SSE interface, MXenes homogenize current and Li^+ flux, lower nucleation overpotentials, suppress voiding, and raise critical current density while providing mechanical shielding against dendrite penetration (see Sections 4 and 6); (ii) as 3D hosts/aerogels or laminar coatings for Li metal, they distribute current and accommodate volume changes, mitigating contact loss; (iii) as low-loading conductive networks in composite cathodes (~2–5 wt%), their sheet-like percolation delivers electronic conductivity without sacrificing volumetric energy density and improves adhesion with SSE particles/binders (Section 3); (iv) as nanofillers in solid polymer or hybrid electrolytes, they decrease polymer crystallinity, promote salt dissociation, create interconnected Li^+ pathways that can push conductivities toward 10^{-3}–10^{-2} S cm^{-1} at modest temperatures, increase Li^+ transference number, and reinforce mechanics for thin membranes (Section 5); and (v) via termination-tunable surfaces (-O/-OH/-F/-Cl), they act as chemical buffers/passivators at reactive interfaces (e.g., Li/sulfide or high-voltage cathode/sulfide), curbing parasitic reactions and stabilizing interphases while maintaining electron/ion continuity (Sections 5 and 6). These roles directly target ionic transport, interfacial resistance, chemical compatibility, mechanical integrity, and cathode-side transport—the very pain points of practical SSBs—thereby clarifying the specific potential of MXenes beyond their general success in liquid-cell systems.

Beyond their direct application as electrodes, MXenes have shown potential in other functional roles within SSB architectures. As conductive additives in cathodes, MXenes can form electronic percolation networks, enhancing conductivity without sacrificing volumetric energy density, outperforming traditional carbon-based additives [20]. As protective layers or host scaffolds for lithium metal anodes, MXenes can suppress dendrite growth due to their mechanical strength and lithiophilic surfaces, improving interfacial stability and safety [11]. Moreover, incorporation of MXenes into solid polymer or composite electrolytes enhances ionic conductivity by promoting segmental motion of polymer chains and creating interconnected pathways for ion transport. Their mechanical reinforcement effect also improves the flexibility and durability of polymer electrolytes [21]. Equally important for translation, MXenes can be deposited from aqueous or polar inks by blade/slot-die coating, spray, or vacuum filtration to form conformal, ultrathin films, enabling roll-to-roll interfacial engineering compatible with large-area SSB components; nonetheless, environmental stability (oxidation/restacking in humid media), scalable synthesis, and cost remain active constraints that we discuss in Sections 7 and 8.

Recent studies have also explored MXene-based interfacial engineering strategies to address high interfacial resistance in SSBs. MXene interlayers between electrodes and solid electrolytes can improve interfacial contact, reduce impedance, and accommodate volume changes during cycling, mitigating mechanical degradation [22]. Their rich surface chemistry allows tailoring of interfacial compatibility through functional group modification or composite formation with sulfide, oxide, or polymer electrolytes [23]. Despite these promising features, challenges remain in terms of MXene scalability, environmental stability (e.g., susceptibility to oxidation in humid environments), and cost-effective integration into battery manufacturing processes [24]. In this review, we aim to provide a comprehensive and critical overview of the multifunctional roles of MXenes in solid-state batteries, maintaining a practical focus: it first summarizes MXene structure, synthesis, and properties relevant to SSBs (Section 2); then examines their use as anodes and conductive additives in cathodes (Section 3), as hosts and protective layers for Li metal (Section 4), and

as functional fillers in solid polymer/composite electrolytes (Section 5); it subsequently details MXene-based interfacial engineering to mitigate resistance and chemical incompatibility (Section 6), before addressing scalability and future directions (Sections 7 and 8). By explicitly linking SSB bottlenecks to MXene-enabled solutions, we provide a clear roadmap for engineering safer, high-performance SSBs.

2. MXenes: Structure, Synthesis, and Properties

2.1. Crystal Structure and Surface Terminations

MXenes are a family of two-dimensional (2D) transition metal carbides, nitrides, or carbonitrides with the general formula $M_{n+1}X_nT_x$, where M denotes an early transition metal (e.g., Ti, V, Nb, Mo), X is carbon and/or nitrogen, and Tx represents surface terminations such as -O, -OH, and -F. These materials are derived by selective etching of the A-group element from their parent MAX phases, $M_{n+1}AX_n$, where A typically belongs to groups 13 or 14 (e.g., Al, Si) [10,25]. The MAX phases exhibit a layered hexagonal structure (space group $P6_3/mmc$) comprising M-X octahedra stacked along the c-axis, with the A atoms interleaved between $M_{n+1}X_n$ slabs. Upon etching, the A-layers are selectively removed, resulting in exfoliated $M_{n+1}X_nT_x$ layers that retain the in-plane crystallinity of the parent phase while introducing surface functional groups (Tx), originating from the etching medium (see Section 2.2 for a concise overview of synthesis routes) [11,26]. In this section, we focus on the structural consequences and notation rather than procedural details. The most studied MXene, $Ti_3C_2T_x$, features a trilayer structure composed of a central carbon layer sandwiched between two titanium layers. After etching, terminations bind to the exposed Ti atoms on the surface, forming Ti-O, Ti-F, or Ti-OH bonds depending on the chemistry and post-treatments employed. High-resolution transmission electron microscopy (HRTEM) and synchrotron X-ray diffraction (XRD) studies have confirmed the presence of well-defined interlayer distances ranging from ~0.9 to 2.0 nm, depending on the nature and amount of surface terminations [27,28] (see Figure 1).

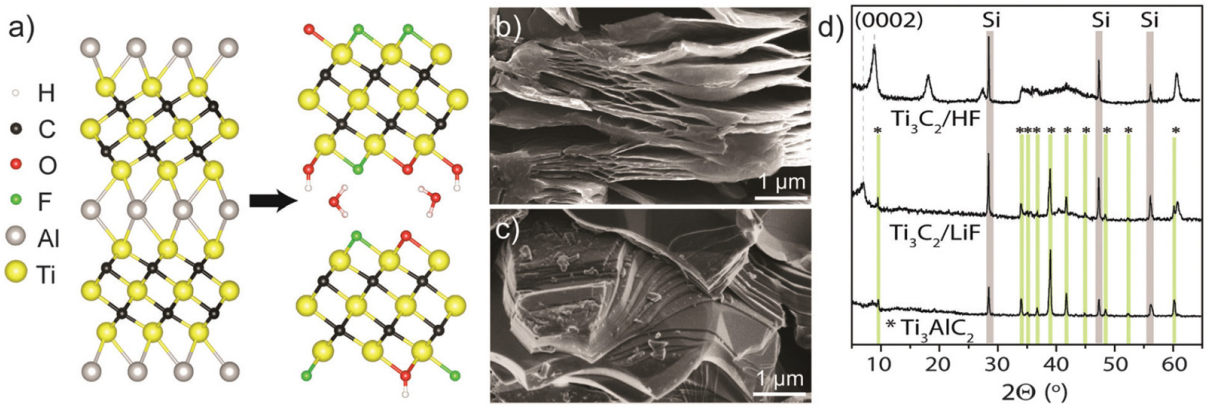

Figure 1. Conversion of Ti_3AlC_2 into $Ti_3C_2T_x$ with surface terminations and interlayer water (**a**); SEM images of $Ti_3C_2T_x$ prepared by HF etching (**b**), showing an accordion-like shape, and LiF-HCl etching (**c**), yielding a more compact form; XRD patterns of Ti_3AlC_2 and $Ti_3C_2T_x$ (**d**); green lines and asterisks mark MAX phase peaks, while grey bands correspond to crystalline Si (10 wt% standard). (Adapted with permission from ref. [28], Royal Society of Chemistry 2016).

Surface terminations critically influence the structural stability and electronic properties of MXenes. Density Functional Theory (DFT) studies show that bare (non-terminated) MXene surfaces tend to be metallic, but oxygen terminations can induce semiconducting behavior by opening a small bandgap, while fluorine and hydroxyl terminations typically preserve metallicity but modify the density of states near the Fermi level [15,29]. These elec-

tronic modifications are strongly dependent on the specific termination sites (top, hollow, bridge) and their distribution across the surface.

Experimentally, X-ray photoelectron spectroscopy (XPS) is widely employed to quantify and identify surface terminations. The relative intensities of Ti-O, Ti-OH, and Ti-F peaks provide insight into the chemical environment of surface atoms and confirm that termination ratios vary substantially with synthesis conditions [30]. Raman spectroscopy and solid-state nuclear magnetic resonance (NMR) further support the structural assignment of functional groups and help track degradation or oxidation over time [31,32]. Importantly, the type and density of surface terminations affect interlayer interactions, spacing, and surface energy. These factors play a decisive role in colloidal stability, mechanical flexibility, and ion intercalation capabilities, which are addressed in later sections. For example, hydroxyl-rich MXenes exhibit enhanced hydrophilicity and swelling in aqueous media, while fluorine terminations lead to more compact structures due to reduced hydrogen bonding potential [33].

Understanding and controlling surface terminations is thus central to tailoring MXene performance across a wide range of applications. In solid-state battery systems, these terminations will later be shown to influence interfacial compatibility, ionic transport, and electrochemical behavior (see Sections 2.3, 4 and 5).

2.2. Synthesis Methods

MXenes are typically synthesized by selectively etching out the A-layer from MAX phases ($M_{n+1}AX_n$), which are layered ternary carbides or nitrides. The choice of etching method (e.g., HF, LiF/HCl, fluorine-free hydrothermal/alkaline, molten-salt) and subsequent delamination/post-treatment steps governs the resulting T_x groups, interlayer spacing, and processability. Before detailing the etching routes, it is worth noting that precursor MAX powders are commonly prepared via conventional high-temperature solid-state synthesis. Typical protocols blend stoichiometric metallic powders with carbon (e.g., Ti, Al, and graphite for Ti_3AlC_2; Nb, Al, and graphite for Nb_2AlC), followed by ball-milling/pelletization and heat treatment at 1300–1500 °C under flowing Ar for 2–4 h (heating rates ~5–10 °C min^{-1}). The consolidated product is subsequently crushed and sieved ($\leq$45–75 μm), and phase purity is verified by X-ray diffraction, consistent with the hexagonal $P6_3/mmc$ structure. Variants employing spark plasma sintering or hot-pressing (≈1100–1400 °C; 20–50 MPa) have also been reported to shorten dwell times while achieving comparable phase purity. Below, we describe the three major synthesis routes: HF etching, in situ acid etching (including fluorine-free methods), and molten salt synthesis.

2.2.1. HF Etching

Hydrofluoric acid (HF) etching is the earliest and most widely used method for MXene synthesis. MAX powders were synthesized as described above. The typical procedure involves immersing powdered MAX phase (e.g., Ti_3AlC_2) in concentrated HF solution (40–50%) at room temperature for 12–48 h. This process removes the A-site atoms (e.g., Al), following the reaction:

$$Ti_3AlC_2 + 3HF \rightarrow Ti_3C_2 + AlF_3 + 1.5H_2\uparrow$$

The product is a multilayered MXene (e.g., $Ti_3C_2T_x$), where T_x represents surface functional groups like -F, -OH, and =O that originate from the HF medium. These terminations are covalently bonded to the surface Ti atoms and play a critical role in tuning hydrophilicity, conductivity, and interlayer spacing [10,11]. To obtain delaminated single- or few-layer MXene sheets, intercalation agents such as dimethyl sulfoxide (DMSO), tetrabutylammonium hydroxide (TBAOH), or Li+ are introduced. This is followed by mild sonication to

overcome the van der Waals forces between MXene layers, resulting in stable colloidal suspensions [33,34]. Despite its effectiveness, HF etching poses significant limitations:

- Toxicity and corrosiveness of HF require stringent safety protocols.
- Environmental hazards due to fluorinated byproducts.
- Limited control over termination chemistry and delamination yield.

For example, $Ti_3C_2T_x$ obtained via HF etching typically exhibits high fluorine content, which may be undesirable for certain applications, such as biomedical systems or devices requiring low electronic impedance [35].

2.2.2. In Situ Acid Etching (Fluorine-Free or Reduced-Fluoride Methods)

To mitigate the hazards associated with concentrated HF, a milder alternative involves generating HF in situ by mixing a fluoride salt (e.g., LiF, NaF, or KF) with hydrochloric acid. This reaction proceeds as:

$$LiF + HCl \rightarrow HF + LiCl$$

This method, pioneered by Ghidiu et al. [36], uses 1 M LiF + 6 M HCl at 35–40 °C for 24 h and yields $Ti_3C_2T_x$ with lower fluorine content and enhanced electrochemical performance. The presence of Li^+ ions facilitates spontaneous intercalation during etching, leading to expanded interlayer distances (often >1.2 nm), which simplifies delamination and promotes ion transport in applications like batteries and supercapacitors [37].

In situ etching methods offer several advantages, including improved safety through the use of milder reagents, better control over the composition of surface functional groups, and a higher yield of delaminated MXenes facilitated by spontaneous intercalation. For example, $Ti_3C_2T_x$ synthesized using a LiF/HCl mixture demonstrates enhanced pseudocapacitive behavior and reduced charge transfer resistance (R_{ct}) compared to MXenes obtained via direct HF etching [17]. Additionally, fully fluorine-free methods are emerging. These typically employ alkaline hydrothermal etching using NaOH, KOH, or LiOH at elevated temperatures (120–200 °C). This produces hydroxyl-terminated MXenes, such as $Ti_3C_2(OH)_x$, without introducing fluorinated residues. Li et al. demonstrated that hydrothermal etching with 10 M NaOH at 180 °C for 48 h effectively removes the Al layer and yields MXenes with promising structural integrity and electrochemical behavior [38]. Although fluorine-free routes are more environmentally friendly, they are still under development and face several limitations, including their applicability to a narrow range of MAX phases (primarily Ti_3AlC_2 and Nb_2AlC), challenges related to incomplete etching or the formation of residual oxides, and limited scalability due to the high temperatures and pressures typically required during synthesis.

2.2.3. Molten Salt Synthesis

Molten salt etching represents a promising HF-free method for MXene synthesis, where MAX phases are exposed to Lewis acidic molten salts such as $ZnCl_2$, $CuCl_2$, or $FeCl_3$ at high temperatures (typically 500–600 °C). Through cation exchange and volatilization of the A-layer, this process yields MXenes with non-fluorinated surface terminations like -Cl, or even with metal decoration [39]. For instance, Wang et al. demonstrated that etching Ti_3AlC_2 with molten $ZnCl_2$ at 550 °C produces $Ti_3C_2Cl_2$, a Cl-terminated MXene exhibiting high electrical conductivity (up to 15,000 S/cm) and enhanced environmental stability [40], thus broadening the scope of MXene surface chemistries beyond traditional -F and -OH terminations. This technique avoids the use of hazardous HF or fluoride salts and offers potential for scalable batch processing, while enabling access to unique surface terminations not achievable through wet chemical routes. Nevertheless, the requirement for elevated

temperatures may restrict compatibility with certain substrates, and there is a risk of phase decomposition or unwanted side reactions. Additionally, thorough post-processing is needed to eliminate residual salts and impurities. Despite these challenges, molten salt synthesis is particularly attractive for producing metal-decorated MXenes and tuning surface chemistry via in situ doping strategies [41].

To aid comparison across synthesis routes, Table 1 summarizes representative conditions (reagents and temperature), the predominant surface terminations (T_x) obtained, and salient implications for processing and interfacial behavior relevant to SSBs.

Table 1. Summary of MXene synthesis routes, terminations and salient properties.

Route	Reagents & Conditions	Phases	Main Terminations (Tx)	Salient Outcomes	Reference
Direct HF etching	Aqueous HF (≈10–50 wt%) at RT-35 °C; 12–48 h; post-washing & intercalation (DMSO, TBAOH, Li^+) for delamination	$Ti_3C_2T_x$ (from Ti_3AlC_2), Nb_2CT_x (from Nb_2AlC), etc.	-F, -OH, -O (fluoride-rich; mixed)	Produces multilayer powders; high conductivity; F-rich surfaces can lower polymer compatibility but aid hydrophilicity.	[42]
In situ HF (LiF/HCl, "MILD")	LiF + HCl (e.g., 1 M/6 M) at 35–40 °C; 12–24 h; spontaneous Li^+ intercalation; easy delamination	$Ti_3C_2T_x$ (highly delaminable "clay")	-OH/-O + reduced -F; Li^+ pre-intercalation	Larger interlayer spacing (often > 1.2 nm) and better processability; high volumetric capacitance.	[36,43]
Fluorine-free alka-line/hydrothermal	Concentrated NaOH/KOH/LiOH(e.g., 27.5–30 M NaOH) at 180–270 °C (autoclave); 15–48 h; fluorine-free	$Ti_3C_2T_x$ (T = OH, O)	-OH, -O (no F)	Improves compatibility; greener route; current scope most mature for Ti- and Nb-MAX; careful control required.	[38,44]
Lewis-acid molten-salt (LAMS)	$ZnCl_2$, $CuCl_2$, etc., 500–800 °C; A-site replacement + etching; HF-free; often yields Cl-terminatedMXenes; subsequent delamination protocols	$Ti_3C_2Cl_2$, Ti_2CCl_2; also Zn-MAX intermediates (Ti_3ZnC_2, . . .)	-Cl (and other halides), sometimes mixed; F-free	Halogen-terminated MXenes with good stability; scalable batches; requires salt removal; high-T processing.	[38,39]

2.3. Physicochemical Properties Relevant to Solid-State Batteries (SSBs)

MXenes exhibit a unique set of physicochemical properties that make them exceptionally well-suited for applications in solid-state batteries (SSBs). These properties—namely, high electrical conductivity, tunable surface chemistry, and excellent mechanical behavior—address many of the limitations encountered with traditional electrode and interfacial materials. Their two-dimensional morphology also allows seamless integration into multilayered battery architectures, enabling structural coherence and minimizing interfacial resistance, which are critical for the performance and durability of SSBs. One of the most outstanding features of MXenes is their metallic or near-metallic electrical conductivity. Pristine $Ti_3C_2T_x$, the most studied member of the MXene family, can reach in-plane conductivities exceeding 15,000 S/cm in its multilayer form and above 20,000 S/cm in delaminated films, depending on processing conditions and termination chemistry [17,27]. This excep-

tional conductivity arises from delocalized d-electrons across the transition metal layers and is preserved even in the presence of surface terminations such as -OH, -F, or -O, albeit with subtle modifications to the density of states near the Fermi level [12,29,45]. Importantly, this high conductivity is maintained even when MXenes are embedded in composite matrices or applied as thin films, enabling their use as both active materials and conductive additives without relying on carbon black or metallic fillers. In the context of SSBs, where solid electrolytes inherently exhibit low ionic conductivities, especially at room temperature, the addition of highly conductive MXene networks can significantly reduce internal resistance and enhance rate performance. Equally critical to MXene performance is their rich surface chemistry, which is intrinsically tied to the synthesis method. Unlike graphene and other inert 2D materials, MXenes naturally bear a variety of functional groups such as -OH, -O, -F, and in some cases -Cl or even metal terminations (e.g., Zn), introduced during HF, LiF/HCl, or molten salt etching processes [33,39]. These functional groups significantly affect electrochemical reactivity, ion accessibility, and interfacial adhesion. For example, hydroxyl- and oxygen-terminated surfaces demonstrate high affinity for Li^+ and Na^+ ions, facilitating fast ion intercalation and enabling pseudocapacitive charge storage behavior [46]. These terminations also impact the wettability of MXene surfaces, improving compatibility with solid polymer electrolytes (SPEs) such as PEO, PAN, or PVDF, and inorganic-polymer hybrid electrolytes. In SSBs, improved wetting promotes intimate electrode-electrolyte contact. Moreover, the presence of polar groups enhances dispersion in polar solvents, allowing solution processing techniques to be used for large-area film fabrication, which is pivotal in scale-up and flexible battery configurations [47]. Beyond their electronic and surface properties, MXenes also demonstrate remarkable mechanical behavior that is advantageous for integration in solid-state devices. Their high in-plane stiffness (with reported Young's modulus values of ~300–500 GPa for $Ti_3C_2T_x$) combines with their nanoscale thickness and flexibility to produce robust, conformal coatings capable of accommodating strain without cracking [26]. When assembled into films, MXenes maintain structural integrity under repeated electrochemical cycling and mechanical deformation, a key requirement for flexible or wearable SSBs. Their lamellar structure also allows interlayer engineering through the intercalation of ions or molecules (e.g., Li^+, DMSO, urea), which can expand the interlayer spacing and reduce ion diffusion barriers. This is particularly relevant for enhancing ionic conductivity in solid electrolytes or improving rate capability in composite electrodes [32,48]. In summary, the physicochemical profile of MXenes—combining metallic conductivity, reactive surface functionality, hydrophilicity, mechanical robustness, and facile processability—enables their versatile application in SSBs as conductive scaffolds, interfacial layers, or redox-active hosts. These attributes make them fundamentally different from most other 2D materials and position them as multifunctional building blocks for next-generation energy storage systems.

2.4. Comparative Advantages over Other 2D Materials (Graphene, MoS_2, BN)

Over the last decade, various two-dimensional (2D) materials have been explored for battery-related applications, each offering unique features. However, when evaluated comprehensively for use in solid-state batteries, MXenes offer a superior combination of properties not found in graphene, transition metal dichalcogenides (TMDs) such as MoS_2, or insulating materials like h-BN. Graphene is often cited for its outstanding electrical conductivity (~10^4 S/cm) and large surface area, but its chemical inertness severely limits its ability to interact with other components in SSBs. To render graphene functional, extensive chemical treatments such as oxidation (producing graphene oxide, GO) and subsequent reduction (rGO) are necessary. These processes introduce defects that deteriorate conductivity and structural integrity. By contrast, MXenes naturally possess a high density of

chemically active sites due to their surface terminations, allowing spontaneous bonding or hydrogen bonding interactions with polymer and inorganic electrolytes [49]. These intrinsic functional groups not only enhance ion transport and interfacial adhesion but also allow for tunable surface properties without the need for harsh post-synthesis modifications. In terms of redox activity and ionic storage capability, MXenes are particularly advantageous over MoS_2. While MoS_2 provides lithium-ion storage through intercalation and conversion mechanisms, it suffers from poor electrical conductivity and significant volume expansion during cycling, which can cause structural degradation. MXenes, on the other hand, operate primarily through intercalation pseudocapacitance with minimal structural changes, allowing for better cycling stability, particularly in the case of $Ti_3C_2T_x$ and Nb_2CTx, which have shown excellent rate capabilities and cycle life in both Li^+ and Na^+ systems [50]. Furthermore, MXenes often exhibit higher volumetric capacity due to their dense packing, a critical metric for practical solid-state devices where volumetric energy density is paramount. h-BN, known for its thermal stability and insulating behavior, has been proposed as a protective interfacial layer in battery systems. However, its lack of electrical conductivity makes it unsuitable as an electrode or conductive additive. MXenes, by contrast, offer similar thermal and mechanical stability while also serving as efficient electron conductors and Li-ion hosts. Additionally, h-BN's non-reactive surface hinders its integration into multi-material systems, whereas MXenes' polar terminations facilitate adhesion and charge transfer across interfaces [51,52]. Processability is another domain where MXenes outperform their 2D counterparts. While graphene, MoS_2, and BN often require surfactants or binders to form uniform films or coatings, MXenes can be dispersed in water or polar solvents without surfactants, yielding stable colloidal solutions. These can be processed into thin films via simple techniques like vacuum filtration, drop-casting, spin coating, or inkjet printing, enabling scalable and uniform deposition for battery electrodes and solid–electrolyte interfaces [37]. This high processability, combined with the tunable thickness and surface chemistry of MXene films, facilitates the formation of continuous, conformal interfacial layers essential for reducing interfacial resistance in SSBs. Taken together, the properties of MXenes—particularly their high electrical conductivity, active surface terminations, redox capacity, mechanical flexibility, and superior processability—combine to offer a multifunctional platform for solving multiple challenges simultaneously in solid-state battery development. Their dual role as both structural and electrochemical components gives them an edge over more limited-functionality 2D materials.

3. MXenes as Electrode Materials

The integration of MXenes into solid-state battery architectures has garnered significant attention due to their unique combination of properties, including high electronic conductivity, tunable surface chemistry, layered morphology, and mechanical flexibility. These features make MXenes promising candidates not only as active anode materials but also as conductive additives or structural components in composite electrodes. Their ability to accommodate alkali-ion intercalation with minimal structural degradation, along with their compatibility with both polymeric and inorganic solid electrolytes, offers strategic advantages in overcoming interfacial and transport limitations commonly encountered in solid-state batteries (SSBs). This section explores the role of MXenes in electrode design, with emphasis on their function as anode materials, their electrochemical performance metrics, and the underlying ion storage mechanisms that govern their behavior in solid-state configurations.

3.1. MXenes as Anodes in Solid-State Batteries (SSBs)

The search for efficient and stable anode materials remains a central challenge in the development of high-performance solid-state batteries (SSBs). In the anode demonstrations reviewed here, we explicitly indicate the solid-state electrolyte (SSE) type for each case—polymer (e.g., PEO-LiTFSI) [53], oxide (e.g., LLZO, NASICON/LATP) [54], sulfide (e.g., LGPS, Li_6PS_5Cl) [55], and halide (e.g., Li_3InCl_6) [56]—because compatibility and MXene's role differ across families: at Li | LLZO, MXenes chiefly lower nucleation overpotential and improve wetting/contact; in sulfides, they also act as electronically conductive yet chemically moderating buffers that curb reductive decomposition; in polymers, they preserve intimate contact and aid void healing under stack pressure; and in halides, they help maintain low-impedance interfaces across a wider cathodic/anodic window. Conventional anodes such as graphite, lithium metal, or silicon face significant limitations when integrated into solid-state configurations due to issues such as poor interfacial contact, limited Li^+ mobility, and severe volume changes during cycling. MXenes have recently emerged as a promising class of 2D transition metal carbides and nitrides that offer a unique combination of metallic conductivity, intercalation pseudocapacitance, and mechanical resilience, which make them particularly suitable as anode materials in SSB systems. One of the primary advantages of MXenes as anodes is their ability to deliver competitive specific capacity through reversible intercalation of Li^+ and Na^+ ions. For example, $Ti_3C_2T_x$ has demonstrated a reversible capacity of ~370 mAh/g in organic liquid electrolytes, which corresponds to the insertion of up to 1 mol of Li^+ per formula unit of Ti_3C_2 [42]. In solid-state configurations, where ion transport is restricted by the rigid electrolyte matrix, $Ti_3C_2T_x$ still exhibits capacities in the range of 150–250 mAh/g depending on the processing conditions, termination groups, and cell architecture [57,58]. The high volumetric capacity of MXenes, stemming from their dense layered stacking (typically >4 g/cm^3), makes them even more appealing for solid-state applications, where space optimization is critical. The cycling stability of MXene-based anodes is also noteworthy. The robust layered structure of $Ti_3C_2T_x$ and its strong Ti-C bonds enable the accommodation of Li^+ insertion/extraction with minimal lattice distortion, reducing the risk of pulverization and mechanical degradation. Several studies have demonstrated that $Ti_3C_2T_x$ retains over 90% of its initial capacity after more than 500 cycles at moderate current densities in SSB configurations using PEO- or $Li_{1.5}Al_{0.5}Ge_{1.5}(PO_4)_3$-based solid electrolytes [59,60]. This cycling stability is further enhanced by the surface functional groups that facilitate Li^+ diffusion across the MXene–electrolyte interface and by the inherent flexibility of MXene nanosheets, which can buffer mechanical stress during repeated cycling. Furthermore, self-healing behavior has been reported in MXene electrodes where cracks formed during cycling are mitigated by van der Waals re-adhesion of neighboring flakes, a phenomenon not typically observed in brittle bulk anode materials [61]. Understanding the mechanisms of Li^+ and Na^+ storage in MXenes is essential to fully leverage their potential in SSBs. In contrast to intercalation in graphite or conversion in metal oxides, MXenes operate via an intercalation pseudocapacitance mechanism—a hybrid behavior that combines fast surface redox reactions with ion intercalation between the layers. This mechanism is characterized by capacitive-like kinetics with diffusion-controlled contributions, which enables rapid charge/discharge and high-rate capability [62]. In situ electrochemical dilatometry and ex situ XRD have shown that Li^+ insertion into $Ti_3C_2T_x$ induces only a modest expansion of ~2–3% in the interlayer distance, allowing for stable structural reversibility [63]. Moreover, DFT calculations and operando spectroscopic techniques (XPS, NMR) have demonstrated that Li^+ ions preferentially bind near surface oxygen or hydroxyl terminations and interact weakly with fluorinated sites, highlighting the importance of termination engineering in optimizing storage behavior [64]. Na^+ storage in MXenes has also gained attention due to

the relevance of sodium-ion SSBs as a cost-effective alternative to lithium-based systems. While the larger ionic radius of Na^+ (1.02 Å) compared to Li^+ (0.76 Å) poses challenges for intercalation, MXenes with expanded interlayer spacing and suitable terminations have been shown to accommodate Na^+ with good reversibility. For example, Na^+ intercalation capacities of ~200 mAh/g and stable cycling over 300 cycles have been reported in $Ti_3C_2T_x$-based solid-state systems using $Na_3Zr_2Si_2PO_{12}$ (NASICON) or Na-β-alumina electrolytes [65,66]. Termination groups play an even more crucial role in Na^+ storage than in Li^+ systems, as hydroxyl-rich surfaces promote stronger ion–surface interactions, enhancing ion retention and suppressing sluggish diffusion kinetics. Additionally, the high electronic conductivity of MXenes eliminates the need for separate conductive additives in the anode composite, simplifying electrode fabrication and reducing interfacial resistance. This is particularly advantageous in SSBs, where the number of interface layers should be minimized to preserve ionic and electronic transport continuity. Some studies have also explored MXene-based hybrid anodes, where $Ti_3C_2T_x$ is combined with Si nanoparticles, Sb_2S_3, or SnO_2 to synergistically combine intercalation and conversion mechanisms, yielding capacities > 500 mAh/g while maintaining good structural integrity [67,68]. In conclusion, the multifunctional character of MXenes—combining fast pseudocapacitive intercalation, high volumetric capacity, cycling robustness, and excellent processability—positions them as highly promising anode materials in the context of solid-state batteries. Their ability to interface directly with solid electrolytes, their tolerance to volume changes, and their tunable surface chemistry allow for flexible electrode design and improved long-term performance. Future directions may include further control of interlayer spacing, exploration of double-transition-metal MXenes for higher capacities, and computational screening of new compositions to enhance Na^+/Li^+ selectivity and transport kinetics in solid-state environments.

3.2. MXenes as Conductive Additives in Cathodes

While MXenes have garnered much attention as active anode materials, their utility extends beyond redox participation. Due to their excellent electronic conductivity, high surface area, and solution-processability, MXenes are increasingly being employed as conductive additives in cathodes for solid-state batteries (SSBs). In these systems, MXenes play a crucial role in constructing electronic percolation networks and promoting synergistic interactions with active cathode materials, thereby enhancing electrochemical performance without sacrificing volumetric or gravimetric energy density. In conventional lithium-ion batteries using liquid electrolytes, conductive additives such as carbon black, Super P, or carbon nanotubes are routinely introduced to ensure sufficient electron transport throughout the composite cathode. However, in solid-state configurations, the challenge is more acute due to the inherently lower ionic and electronic conductivity of many solid electrolytes, combined with rigid electrode structures that can hinder particle connectivity. Here, MXenes offer distinct advantages. Their metallic conductivity (up to ~20,000 S/cm), combined with a 2D sheet-like morphology, allows them to form interconnected conductive networks throughout the cathode, even at very low loadings (~2–5 wt%), significantly outperforming traditional carbon additives in maintaining electronic percolation [42,69]. These percolative networks reduce the electronic resistance of the cathode and facilitate rapid charge transport, especially under high-rate conditions or in thick electrodes designed for high energy density. Unlike spherical or fibrous carbon additives that often require random packing to establish percolation thresholds, MXene sheets can align or interpenetrate active material particles, creating continuous charge transport pathways that bridge isolated regions of the electrode. Moreover, their high aspect ratio and flexibility allow them to conform to the geometry of the surrounding particles and interface

intimately with the solid electrolyte, promoting compact and homogeneous electrode structures [36]. For cathode composites, we name the paired SSE in each example: oxide matrices (LLZO, LATP/NASICON), sulfides (e.g., Li_6PS_5Cl argyrodite or LGPS), and halides (e.g., Li_3InCl_6) [70]. In oxides/halides, MXene sheets primarily build low-loading electronic percolation without penalizing volumetric energy density; in sulfides, they additionally temper interfacial reactivity at high voltage and help maintain a stable CEI while preserving ionic pathways [70]. At $\geq$4.2–4.5 V, the cathode-electrolyte chemistry governs how MXene sheets should be deployed: with oxide SSEs (LLZO/LATP) the challenge is mainly mechanical/contact—MXenes supply low-loading percolation and adhesion without narrowing the ESW [70]; with sulfides (LGPS, Li_6PS_5Cl), oxidative instability at layered oxides (e.g., LCO/NMC) necessitates MXene use as chemically moderating, conformal networks and/or hybridized (MXene@oxide/polymer) interfaces that decouple electronic percolation from direct sulfide contact [70]; with halides (Li_3InCl_6), broader anodic stability allows MXene networks to operate at high voltage provided that surface terminations are tuned to avoid parasitic redox [70].

Beyond conductivity enhancement, synergistic effects between MXenes and cathode active materials have been reported, particularly in layered oxides and conversion-type materials. For instance, $Ti_3C_2T_x$ incorporated into $LiFePO_4$ (LFP) composite cathodes not only improved conductivity but also enhanced Li^+ diffusion kinetics by stabilizing the electrode–electrolyte interface and suppressing polarization, resulting in higher rate capability and better capacity retention [4]. In other studies, MXenes blended with high-voltage cathode materials such as $LiCoO_2$ or $LiNi_{0.8}Co_{0.1}Mn_{0.1}O_2$ (NCM811) improved cycling performance by mitigating interfacial degradation and promoting mechanical cohesion within the electrode layer [5]. These effects are attributed to the interfacial compatibility of MXenes, enabled by their surface terminations (-OH, -O, -F), which can form hydrogen bonds or electrostatic interactions with the cathode particles or solid electrolyte components. Furthermore, DFT calculations suggest that MXenes can act as electron-rich substrates, promoting surface redox reactions and stabilizing the cathode–electrolyte interface under high-voltage operation [6]. Another critical benefit of MXenes in cathode composites is their potential to reduce the amount of inactive material. Conventional carbon additives, while electronically conductive, do not participate in charge storage and occupy space that could otherwise be filled with energy-storing material. Because MXenes can provide both electrical connectivity and partial capacitive contribution, their inclusion may enable more compact electrode designs with higher energy density. Additionally, MXenes show excellent adhesion properties, which improve the mechanical integrity of composite cathodes under the stress of cycling and temperature fluctuations in SSBs [71,72].

The processability of MXenes also contributes to their appeal as conductive additives. Their stable aqueous dispersions enable facile integration with cathode slurries through solution-based processing techniques such as blade coating, vacuum filtration, or inkjet printing. This is particularly advantageous for the fabrication of thick or multi-layered cathodes in solid-state architectures, where uniform dispersion and adhesion to the solid electrolyte are essential to ensure electrochemical and mechanical stability over long-term operation [73]. In summary, the inclusion of MXenes as conductive additives in solid-state cathodes offers multiple performance benefits: superior electronic percolation, improved interfacial contact, enhanced Li^+ transport kinetics, and better structural integrity. These multifunctional roles enable the design of high-energy, high-rate solid-state batteries with improved long-term stability. As such, MXenes represent a powerful alternative to traditional carbon-based conductive agents and pave the way toward more efficient and integrated cathode architectures.

3.3. MXene-Based Composites for Enhanced Electrode Performance

In the realm of solid-state batteries (SSBs), MXenes demonstrate enhanced electrode functionality not only in pure form but, crucially, when integrated into composite architectures. By combining MXenes with complementary materials—such as chalcogens, silicon, selenium, and conversion-type compounds—researchers have developed MXene-based composites that deliver synergistic gains in capacity, rate performance, mechanical stability, and interfacial behavior. One notable example is the Se@MXene composite cathode for all-solid-state Li-Se batteries. In this architecture, selenium nanocrystals are homogeneously distributed within the interlaminar spaces and surfaces of Ti_3C_2 MXene via a novel melt-diffusion approach. Such Se@MXene cathodes achieve high specific capacity (~632 mAh g^{-1} at 0.05 A g^{-1}), outstanding rate capability (up to 4 A g^{-1}), and excellent cycling stability over 300 cycles at 1 A g^{-1} [46,74] (see Figure 2). The performance stems from structural reinforcement by the conductive MXene layers, which preserve electrode integrity during redox transitions between Se and Li_2Se, and ensure electron percolation throughout the solid-state matrix [74].

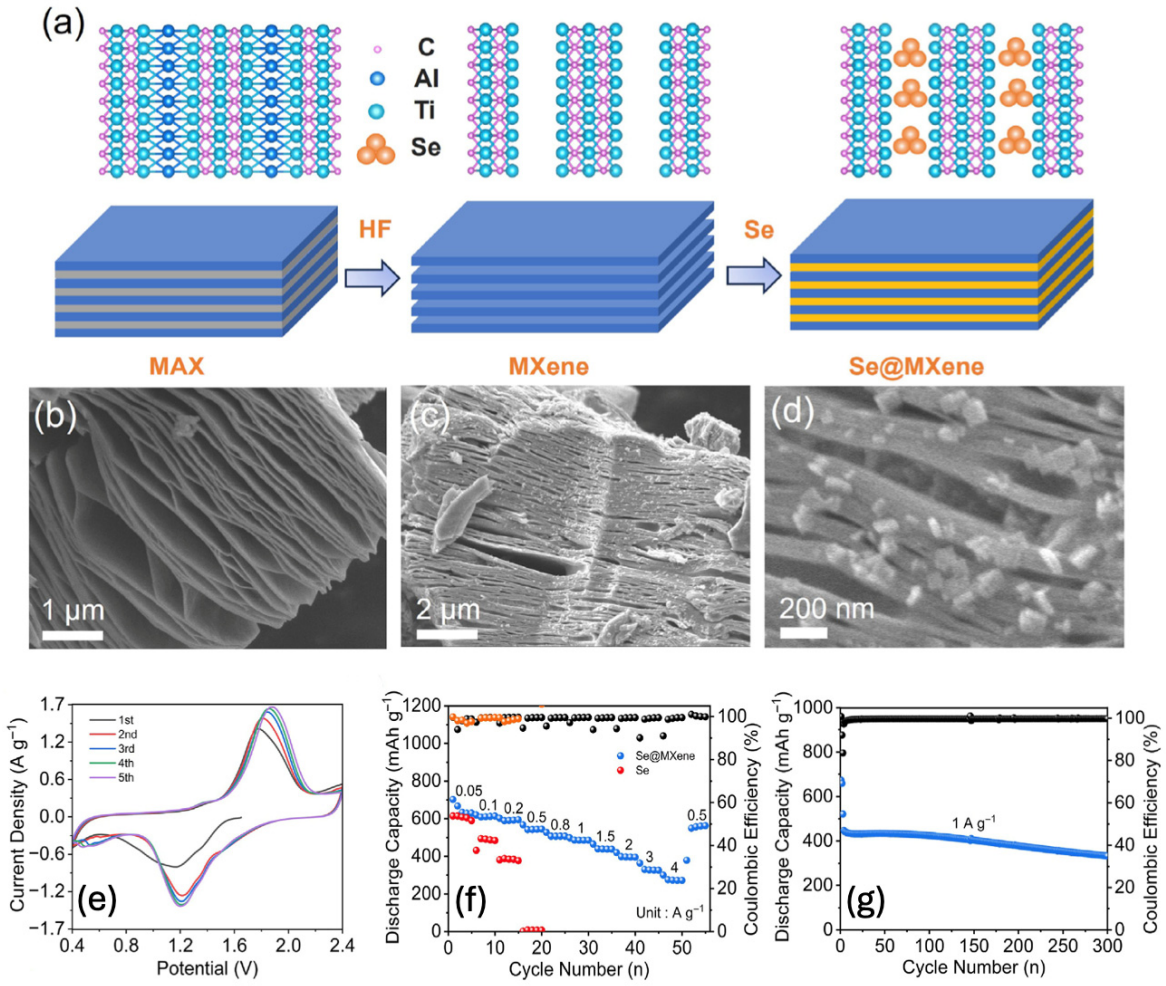

Figure 2. (**a**) Schematic representation of the preparation steps for the Se@MXene composite. SEM micrographs of (**b**) pristine $Ti_3C_2T_x$ layers and (**c**,**d**) Se@MXene, showing the morphological transformation after selenium incorporation. Electrochemical performance of the Se@MXene cathode in a solid-state Li-In/Li^+ cell operating between 0.4 and 2.4 V: (**e**) cyclic voltammetry at 0.2 mV s^{-1}, (**f**) comparison of specific capacities of Se@MXene versus pure Se at different current densities, and (**g**) cycling stability evaluated at 1 A g^{-1}. (Adapted with permission from ref. [74], Elsevier 2024).

In a different class of composites, Si/MXene nanocomposites have been explored to overcome the challenges of silicon anodes—namely, poor electronic conductivity and large volumetric expansion. Recent work reviews the strategies for fabricating Si/MXene composites, where MXene layers serve as conductive hosts and flexible buffers that mitigate silicon's mechanical stress during cycling [75]. Experimental results support that MXene-enhanced silicon electrodes achieve higher reversible capacity, better cyclability, and improved rate capability compared to silicon-alone electrodes [76]. Beyond Si and Se, hybrid MXene composites with conversion-type active materials also show exceptional electrochemical performance. For instance, a VM–MXene hybrid nanostructure—where a MXene backbone supports vanadium-derived active material—exhibits a high initial specific capacity (~460 mAh g^{-1} at 0.1 A g^{-1}) and retains respectable performance (~290 mAh g^{-1}) even at 1 A g^{-1} [77]. These results highlight the dual role of MXenes as electron-conducting frameworks and structural stabilizers. Moreover, MXene composites have been leveraged to improve rate-capacitive behavior in systems requiring fast kinetics. An example includes porous MXene structures engineered via mild chemical oxidation to introduce nanoscale porosity, achieving a porous MXene (PM) anode with high-rate capability: 247 mAh g^{-1} at 0.1 A g^{-1} and 114 mAh g^{-1} at 10 A g^{-1}, with outstanding long-term cycling stability (>1000 cycles at 5 A g^{-1}), particularly in sodium-ion systems [78]. In contrast, the application of MXene composites in cathodes such as quasi-solid-state lithium-iodine batteries demonstrates how MXene layers—when combined with catholyte materials—enable high energy/power densities, stable cycling, and robust electrode integrity under semi-solid-state conditions [79]. Collectively, these studies illustrate that MXene-based composites boost electrode performance through multiple synergistic effects:

- Conductive scaffolds that reinforce electron and ion transport paths;
- Structural buffering that accommodates active material expansion and mechanical strain;
- Enhanced redox kinetics by providing accessible electroactive surfaces;
- Improved interface chemistry in solid-state configurations.

Such composites extend the practical utility of MXenes beyond standalone anodes or additives, positioning them as foundational components in high-performance SSB electrode design.

4. MXenes for Metal Anode Protection and Dendrite Suppression

The implementation of metallic lithium and sodium anodes in solid-state batteries (SSBs) holds tremendous promise for achieving ultrahigh energy densities, owing to their low electrochemical potentials and exceptionally high specific capacities. However, the full realization of these benefits remains elusive due to severe interfacial challenges—most notably, the growth of metal dendrites that compromise safety and cycling stability. Dendritic protrusions can propagate through even rigid solid electrolytes, triggering internal short circuits and catastrophic failure. This issue arises from a combination of factors, including interfacial instability, void formation during stripping, current density inhomogeneities, and the presence of microstructural defects in the electrolyte. Overcoming these obstacles requires materials that can effectively regulate ion deposition, suppress filament growth, and maintain intimate contact between the metal anode and the solid electrolyte throughout extended cycling. MXenes, with their distinctive two-dimensional structure, metallic conductivity, high mechanical strength, and tunable surface chemistry, have emerged as promising candidates to address these challenges. Their ability to serve as protective interfacial layers, dendrite-blocking coatings, or host matrices for metal anodes opens new opportunities to stabilize metal–electrolyte interfaces, promote uniform ion flux, and mechanically suppress dendritic intrusion. This section explores the multifaceted roles

of MXenes in mitigating dendrite formation in SSBs, beginning with an overview of the underlying mechanisms of dendrite growth and followed by strategies involving MXenes as protective coatings and structural hosts.

4.1. Challenges of Dendrite Growth in Solid-State Batteries (SSBs)

The integration of lithium (Li) or sodium (Na) metal anodes into SSBs offers tremendous potential due to their high theoretical capacities (3860 mAh g^{-1} for Li and 1160 mAh g^{-1} for Na) and low electrochemical potentials. However, the formation and propagation of metal dendrites, filament-like structures that penetrate the solid electrolyte, remain one of the most critical limitations to their widespread implementation. Initially, solid electrolytes were expected to mechanically suppress dendrites due to their high elastic moduli. According to the Monroe–Newman criterion, dendrite suppression is possible if the solid electrolyte has a shear modulus at least twice that of lithium metal [80]. Yet, empirical studies have shown that even rigid electrolytes such as garnet-type LLZO and sulfide-based $Li_{10}GeP_2S_{12}$ (LGPS) can still permit dendrite growth under certain conditions [5,81]. This discrepancy arises due to a variety of microstructural and interfacial factors. One major challenge is interfacial instability, particularly void formation during lithium stripping. As lithium is removed from the anode, poor contact with the solid electrolyte leads to regions of high local current density during subsequent plating. This current focusing triggers dendrite nucleation and growth, even at low global current densities, when the critical current density (CCD) is locally exceeded [82,83]. Another key mechanism is grain boundary and defect-mediated growth. In polycrystalline electrolytes, lithium prefers to migrate along grain boundaries or through microcracks and pores, pathways that are mechanically weaker and offer less resistance to dendrite penetration [84]. These defects serve as initiation points for filament formation and compromise the integrity of the electrolyte over time. The mismatch in mechanical properties and interfacial chemistry between the Li metal and solid electrolyte further exacerbates dendrite propagation. Differences in thermal expansion coefficients and mechanical moduli induce stress accumulation at the interface during cycling. These stresses can cause delamination, interfacial degradation, and a rise in cell impedance [85]. Recent operando and cryo-microscopy studies have visualized dendrite nucleation and penetration in real-time. Synchrotron X-ray tomography and cryo-FIB/SEM have confirmed that voids and cracks precede dendrite growth and are correlated with the loss of interfacial contact and mechanical cohesion [86,87]. In the case of sodium metal, the challenges are even more pronounced. Due to its larger ionic radius and lower melting point, Na exhibits worse interfacial wetting and increased susceptibility to non-uniform deposition. Fewer chemically stable solid electrolytes exist for Na systems, making interfacial engineering an even more pressing challenge [88]. In summary, the challenges associated with dendrite growth in SSBs include:

- Interfacial void formation during stripping and plating;
- Current density heterogeneity and local overpotentials;
- Mechanical stress accumulation and interfacial delamination;
- Defect-assisted propagation through grain boundaries and pores;
- Electrochemical instability and formation of resistive interphases;
- Low critical current density thresholds, often below 1 mA cm^{-2} in practice.

These multifactorial limitations highlight the urgent need for advanced interfacial engineering strategies. Materials capable of homogenizing current distribution, maintaining interfacial contact, and blocking dendritic intrusion, such as 2D materials like MXenes, are promising solutions. Their specific roles in this context are addressed in the following sections.

4.2. MXenes as Protective Layers

The application of protective interfacial layers has emerged as a critical strategy to mitigate dendrite formation in solid-state batteries (SSBs) employing lithium metal anodes. These artificial coatings aim to enhance interfacial stability, regulate lithium-ion flux, and mechanically suppress dendritic growth. Among various candidate materials, MXenes have shown exceptional promise due to their metallic conductivity, high mechanical stiffness, tunable surface chemistry, and excellent processability. Recent studies have demonstrated the effectiveness of MXene-based coatings in constructing robust artificial solid–electrolyte interphases (SEIs) or interlayers. For example, Liu et al. engineered a three-dimensional current collector by integrating $Ti_3C_2T_x$ MXene with boron nitride (BN) on a copper substrate [89]. During repeated lithium plating and stripping, a uniform interphase rich in Li_3N and LiF was generated at the MXene-BN/Cu interface, which accommodated volume changes and effectively blocked dendritic growth. This design enabled more than 500 highly stable cycles with a Coulombic efficiency of approximately 98%, even under high current densities. Figure 3 displays representative in situ optical microscopy images comparing Li^+ deposition on MXene-BN with that on 3D Cu foam, clearly showing homogeneous coverage on the MXene surface and the absence of pronounced dendrite formation. These observations demonstrate that the synergistic effect of MXene and BN promotes uniform nucleation, effectively suppressing dendrite formation and enhancing interfacial stability in lithium metal anodes. In oxide garnets (LLZO), ultrathin MXene interlayers promote LiF-rich, low-impedance contacts and homogenize the interfacial field; in sulfide SSEs (e.g., LGPS, Li_6PS_5Cl), MXenes serve as electronically conductive yet chemically buffering layers that mitigate reductive decomposition while maintaining ion access; in polymer SPEs (e.g., PEO-LiTFSI), they enhance wetting and preserve contact/void healing under stack pressure; and in halide electrolytes (e.g., Li_3InCl_6), they help sustain interfacial stability across wider potential windows [90].

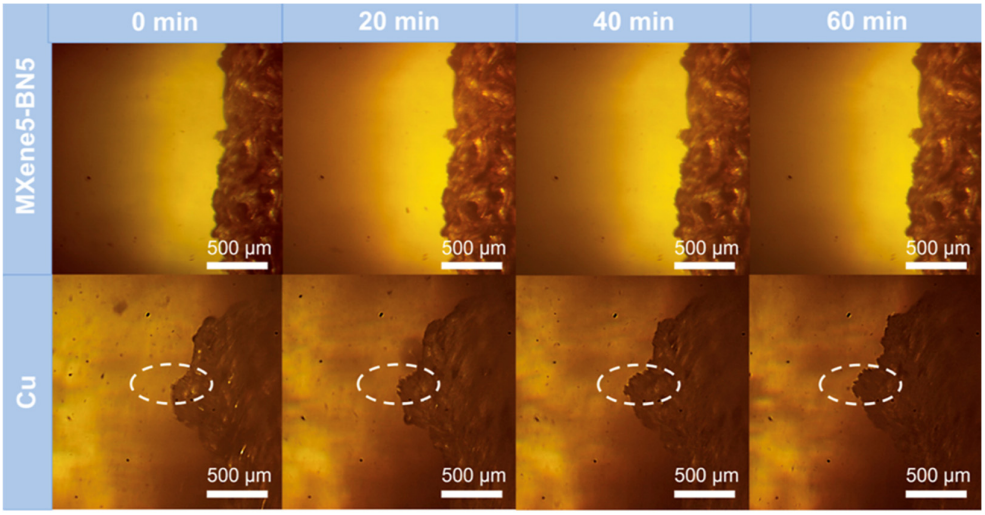

Figure 3. In situ optical microscopy images comparing Li plating and stripping on MXene-BN and bare Cu substrates at different time intervals. While lithium deposition on Cu leads to uneven growth and the formation of dendritic structures (highlighted by dashed circles), the MXene-BN hybrid surface enables homogeneous Li distribution and smooth interface evolution over 60 min. (Adapted with permission from ref. [89], ACS 2023).

In another approach, Wang et al. introduced a dual-protective interface combining MXene nanosheets with covalent organic frameworks (COFs). This composite design leverages the rigidity of MXene and the softness of COFs to create a structurally compliant yet mechanically robust buffer layer. The hybrid layer provided aligned ion-conductive

channels and suppressed lithium dendrite growth by homogenizing the Li^+ flux and alleviating interfacial stress. The resulting full cells exhibited improved cycling performance and reduced impedance evolution over extended cycling [91]. Mechanistically, MXenes function through multiple dendrite-inhibiting pathways:

- Uniform Li^+ flux distribution: The polar surface terminations of MXenes (e.g., -O, -OH, -F) act as lithiophilic sites, lowering the nucleation barrier for lithium deposition and facilitating uniform plating beneath the coating.
- Mechanical suppression: Due to their high Young's modulus (~300–500 GPa), MXene layers can physically resist dendrite protrusion, acting as a mechanical shield without impeding ionic transport.
- Electric field regulation: The excellent electronic conductivity of MXenes helps to redistribute local current densities at the Li–electrolyte interface, thereby mitigating field inhomogeneities that often trigger dendrite nucleation.
- Chemical stability: MXene-based interlayers are relatively inert in contact with both lithium metal and solid electrolytes, reducing interfacial side reactions and preserving long-term interfacial integrity.

Beyond generic contact or conductivity arguments, MXenes suppress dendrites through complementary, mechanism-level effects: (i) lithiophilicity and reduced nucleation overpotential -O/-OH/-F (and -Cl) terminations provide low-barrier Li adsorption sites, homogenizing Li^+ flux and favoring dense, uniform nuclei; (ii) electric-field homogenization—high electronic conductivity turns MXene sheets into quasi-equipotential planes that smooth interfacial "hot spots," lowering current spikes that trigger filament growth; (iii) ultrathin mechanical confinement—stiff, tough films deflect or blunt protrusions while remaining ion-permeable; (iv) in situ interphase chemistry—terminations promote LiF-rich or Li_2TiO_3-like species that reduce impedance and stabilize μLi, curbing parasitic decomposition; and (v) reduced interfacial tortuosity—conformal laminar coatings fill micro-asperities and shorten the effective Li^+ path, thereby raising the stable critical current density. These electrochemical, electronic, mechanical, and chemical contributions explain the consistent dendrite suppression observed for MXene interlayers in SSBs [92–95].

Furthermore, stoichiometrically engineered $Ti_3C_2T_x$ coatings have been used directly on lithium metal surfaces or on current collectors to pre-condition nucleation sites and stabilize initial lithium deposition. These coatings act as artificial SEIs that preemptively form a conformal, ion-permeable protective layer, avoiding the uncontrolled growth of native SEI and inhibiting dendrite evolution [96]. Altogether, MXene-based protective layers represent a powerful platform to control lithium deposition behavior in solid-state batteries. Their combination of lithiophilicity, mechanical strength, and electrochemical stability positions them as multifunctional interfacial materials capable of dramatically extending the cycle life and safety of Li-metal SSBs.

4.3. MXenes as Hosts for Metal Anodes

Achieving stable and dendrite-free metal anodes in solid-state batteries (SSBs) demands more than just protective coatings—it requires thoughtful structural host design. While the interfacial mechanisms are detailed in Section 4.2, MXene hosts provide additional, host-specific effects: (i) continuous 3D conductive networks redistribute current density away from hotspots; (ii) engineered inter-lamellar spacing offers low-tortuosity Li^+ pathways and guides deposition within the scaffold; (iii) capillary/meniscus-assisted wetting promotes Li infiltration into pores, reducing surface protrusions; and (iv) compliant yet resilient frameworks accommodate Li volume change under stack pressure, preserving contact and healing voids during stripping—together delaying interfacial instability and increasing the attainable critical current density [89,91,93,96]. MXenes, with their layered

architecture, exceptional conductivity, modifiable surface chemistry, and mechanical resilience, are emerging as a sophisticated class of scaffolding materials that accommodate metal deposition, buffer volumetric changes, and sustain cycling robustness. One inspiring example involves 3D MXene aerogel scaffolds. These porous, self-supporting networks possess abundant lithiophilic sites—thanks to their surface dipoles—and offer pathways that guide uniform lithium ingress and deposition. Such architecture significantly mitigates volume expansion during cycling and dramatically curtails dendrite formation, enabling high-rate performance in Li metal systems [97,98]. Likewise, scaffolds incorporating MXene/rGO hybrids have demonstrated galvanic synergy between MXene conductivity and graphene flexibility. These conductive frameworks provide homogenous electron pathways and buffer mechanical strain, resulting in smooth Li plating across the host matrix [99]. Another compelling structural innovation centers on MXene–COF composite hosts. By interlacing rigid MXene sheets with soft but ordered, porous COF spheres, researchers crafted a host that merges mechanical strength with ionic accommodation. The COF micropores serve as ion channels and buffer zones, while MXene components ensure electrical percolation and structural stability. Full cells with these hybrid hosts displayed uniformly dense lithium deposition and excellent cycling performance [97]. Chemically functionalizing MXenes to act as artificial solid–electrolyte interfaces (SEIs) on lithium surfaces is another potent approach. Stoichiometric $Ti_3C_2T_x$ coatings enhance lithiophilicity, reduce nucleation overpotentials, and encourage homogeneous deposition by predefining favorable nucleation sites [100]. Collectively, these structural host strategies offer multiple electrochemical performance enhancements. The scaffolds distribute current density over larger surface areas, markedly lowering local currents and suppressing dendrite initiation. Their intrinsic conductivity minimizes reliance on additional conductive additives, streamlining electrode architecture while maintaining rapid charge/discharge dynamics. Mechanically robust but flexible frameworks accommodate volumetric stress, preserving interfacial integrity and curbing impedance growth. Moreover, the tunable nature of MXenes allows interlayer spacing optimization for ion transport and supports straightforward integration into manufacturing-friendly formats like freeze-cast composites, printable inks, or freestanding films. This processability supports scalable production of high-performance SSB anodes.

5. MXenes in Solid Electrolytes

Solid electrolytes are key enablers of next-generation all-solid-state batteries (SSBs), offering safer, more stable ionic transport compared to liquid counterparts. Among them, composite solid polymer electrolytes (SPEs) represent a compelling balance of flexibility, processability, and electrochemical performance. Here, we explore how MXenes, two-dimensional transition metal carbides/nitrides with fascinating structural and surface properties, enhance SPE functionality. In this section, we focus on their role as nanofillers to boost ionic conductivity and as mechanical reinforcements that elevate SPE robustness.

5.1. MXenes in Solid Polymer Electrolytes (SPEs)

Solid polymer electrolytes (SPEs, exemplified here by PEO-LiTFSI and related PEO/SN matrices) have long been recognized for their potential to replace flammable liquid electrolytes in next-generation solid-state batteries owing to their inherent safety and mechanical flexibility. Nevertheless, issues such as low room-temperature ionic conductivity and limited mechanical strength have hindered their practical deployment. The incorporation of MXenes—two-dimensional transition metal carbides and nitrides with high surface area, hydrophilic terminations, and excellent electrical conductivity—has emerged as a transformative approach. When dispersed within polymer matrices such as poly(ethylene oxide) (PEO), MXenes can simultaneously address ionic transport limitations and mechanical

fragility. Early pioneering work by Pan et al. introduced $Ti_3C_2T_x$ MXene nanosheets into a PEO/LiTFSI matrix using a green, aqueous blending approach. At a loading as low as 3.6 wt%, the MXene fillers effectively disrupted PEO crystallization, promoted amorphous regions, and enhanced segmental chain dynamics. These changes led to a remarkable rise in ionic conductivity to around 2.2×10^{-5} S cm^{-1} at room temperature, substantially outperforming composites with zero- or one-dimensional fillers. Even a modest 1.5 wt% of MXene resulted in full cells with rate performance and stability matching state-of-the-art SPE-based lithium-metal batteries [53]. More recently, Xu et al. reported a composite SPE combining PEO and succinonitrile (SN) with MXene fillers, achieving ion conductivities as high as 2.17×10^{-3} S cm^{-1} at 35 °C, a dramatic improvement that brings SPEs closer to practical operating conditions [60]. These enhancements are attributed to the multifunctional role of MXenes: their polar surface terminations aid in salt dissociation, their planar morphology fosters extended amorphous domains, and they may create fast conductive pathways within the polymer matrix. MXenes also significantly bolster the mechanical properties of SPEs. A standout example is a "sandwich" structure where PEO-based SPE is reinforced with $Ti_3C_2T_x$ MXene within a glass-fiber cloth support. This composite demonstrates a tensile strength of 43.4 MPa, more than twelve times that of pristine PEO, and a Young's modulus reaching 496 MPa, over sixtyfold higher, while doubling ionic conductivity at 60 °C to 5.01×10^{-2} S m^{-1}. Lithium symmetric cells using this composite electrolyte exhibited stable cycling for over 800 h, and full cells maintained robust capacity across temperatures from 25 to 60 °C [101]. These dramatic improvements reflect the "stiffness confinement effect," where rigid fillers constrain polymer chain mobility near interfaces, enhancing both mechanical stiffness and dimensional stability [102]. Additionally, MXenes are easily processed via solution methods, enabling scalable manufacturing of thin-film or laminated SPEs. Their hydrophilic surfaces and layered morphology enable uniform dispersion in polar solvents, preventing aggregation and preserving both mechanical flexibility and ionic pathways. Finally, several synergistic mechanisms underpin the simultaneous improvement in ionic transport and mechanical strength. MXenes reduce crystallinity and activate more mobile polymer domains; their polar surfaces facilitate Li^+ dissociation; they serve as structural reinforcements that resist deformation; and their conductive pathways enhance interfacial stability with electrode materials, potentially lowering interfacial impedance. Mechanistically, MXenes increase ionic conductivity (σ) and the Li^+ transference number (t^+) in SPEs via: (i) Lewis interactions and termination-assisted salt dissociation, promoting salt dissociation and partial anion immobilization, which elevates t^+ and reduces polarization; (ii) reduced polymer crystallinity and faster segmental motion—sheet–polymer interactions (e.g., with PEO, PAN, PMMA) disrupt crystalline domains and facilitate Li^+ hopping; (iii) 2D transport pathways and Maxwell–Wagner–Sillars interfacial polarization—permittivity-contrast microdomains at MXene/polymer interfaces channel Li^+ migration, while partially spaced 2D planes act as "ion highways" when restacking is controlled; and (iv) "fine" mechanical reinforcement—higher membrane modulus allows thinner films and lower area-specific resistance without sacrificing puncture resistance. Net effect: higher apparent σ, higher t^+, and lower interfacial impedance, translating into improved high-current response in SSB cells [53,103–105].

5.2. MXenes in Inorganic/Polymer Composite Electrolytes

Composite solid electrolytes that combine inorganic fillers (oxide LLZO/LLZTO, NASICON/LATP; sulfides such as LGPS or Li_6PS_5Cl; and halides such as Li_3InCl_6) with polymer matrices represent a promising strategy for achieving solid-state electrolytes that are both ionically conductive and mechanically robust. These hybrid systems aim to leverage the high mechanical modulus and ionic conductivity of ceramic fillers, while main-

taining the processability and flexibility of polymers such as PEO or PVDF. In this context, MXenes have emerged as particularly effective multifunctional additives. Their layered morphology, metallic conductivity, and rich surface functionalization (-O, -OH, -F) make them uniquely suited to promote long-range ion transport and to improve interfacial and structural stability under operating conditions. One of the most impactful contributions of MXenes to these hybrid systems lies in their ability to form efficient and continuous ionic pathways. This is accomplished through several synergistic mechanisms: MXenes reduce polymer crystallinity, enhance the dissociation of lithium salts, and promote segmental mobility. Furthermore, their surface terminations act as Lewis bases that interact strongly with Li^+, effectively increasing the Li^+ transference number and promoting faster ion migration across the bulk and interfacial regions. For example, Yang et al. demonstrated that MXene-based polymer composites—specifically PEO/LiTFSI with 2D $Ti_3C_2T_x$—displayed higher ionic conductivity and reduced activation energy due to improved chain mobility and anion immobilization, with conductivities reaching up to 10^{-3} S cm^{-1} at 30 °C [103]. Another notable case is the incorporation of MXene quantum dots (MX-QDs) into starch-acetate-based solid polymer matrices. In a recent study by Hadad et al., the click-chemistry-assisted composite showed a record ionic conductivity of 14.8 mS cm^{-1}, a lithium-ion transference number of 0.91, and an electrochemical stability window of 5.2 V. These exceptional values were achieved with only 0.4 wt% MX-QD content, attributed to the formation of percolating anion migration networks and uniform Li^+ flux regulation across the membrane. Most importantly, full cells using this composite retained 90% of their capacity after 1000 cycles, even under elevated temperatures—strong evidence of the operational stability imparted by MXene-based architecture [106]. The mechanical reinforcement imparted by MXenes is also critical to the performance of inorganic/polymer hybrid electrolytes. A study by Likitaporn et al. reported on electrospun PAN/polyurethane (PU) membranes enhanced with $Ti_3C_2T_x$ MXenes, which showed a 2214% increase in electrolyte uptake, thermal stability up to 180 °C, and ionic conductivity of 3.35×10^{-3} S cm^{-1}. These membranes not only showed superior dimensional and thermal integrity under operational conditions but also enabled uniform lithium plating/stripping over 500 h in symmetric cell configurations without dendrite formation [107]. MXenes also contribute to the long-term environmental and chemical stability of solid electrolytes. A multi-year aging study by Lee et al. examined $Ti_3C_2T_x$ MXene films stored under ambient conditions for 4 to 9 years. Remarkably, even after such prolonged exposure, the MXene structures retained a large fraction of their electrical conductivity, and their electrochemical performance could be restored via simple vacuum annealing. This level of resilience suggests that MXenes may play a vital role in improving the durability and manufacturability of solid-state battery electrolytes, particularly for devices exposed to ambient processing environments or prolonged storage [108]. In hybrid composites, MXenes operate synergistically with ceramic fillers: their high surface charge density and tunable terminations improve particle–binder adhesion and wetting, create continuous percolation routes that shorten Li^+ paths across grains/binders, and buffer acid–base mismatches at sulfide/oxide–polymer interfaces—thereby limiting resistive interphase growth. At sub-percolation loadings (~0.5–5 wt%), aligned sheets deliver conductivity gains without compromising mechanical integrity, especially when interlayer spacing is stabilized by polymeric or nanoparticulate spacers to prevent restacking [53,60,105].

Taken together, these findings affirm that MXenes serve as more than passive fillers: they actively engineer ion transport networks, enhance mechanical resilience under strain, and ensure long-term stability in chemically demanding environments. Their versatility as nanostructured additives in inorganic/polymer composite electrolytes makes them an indispensable component in the roadmap toward high-performance, flexible, and durable all-solid-state lithium batteries.

5.3. Impact on Electrochemical Stability Window and Interfacial Compatibility

The effectiveness of electrolyte materials in solid-state batteries (SSBs) hinges not only on their ionic conductivity and mechanical stability, but critically on two interrelated factors: their ability to maintain a wide electrochemical stability window (ESW)—enabling compatibility with high-voltage cathodes and reactive anodes—and their capacity to form robust interfaces with electrode materials, which minimize impedance and suppress electrochemical degradation over cycling. MXenes have demonstrated unique advantages in both areas. Thanks to their chemically inert surface terminations (-O, -OH, -F) and tunable work function, they remain stable within broad voltage ranges. For instance, Wang et al. developed a multifunctional MXene-bonded conductive network embedded in a polymer electrolyte for solid-state zinc batteries. This network maintained electrochemical stability across a wide voltage range while supporting high-rate cycling, highlighting MXene's chemical resilience under demanding electrochemical conditions [50]. For high-voltage layered oxides (LCO/NMC) paired with sulfide SSEs, MXenes are most effective as ultrathin, electron-conducting yet chemically buffering interlayers (or as "encapsulated" percolation networks) that limit sulfide oxidation and stabilize the CEI; with oxide SSEs (LLZO/LATP), their primary role is to reduce electronic tortuosity and improve cohesion without compromising the anodic window; with halide SSEs (Li_3InCl_6), the wider anodic stability enables low-loading percolation in thick cathodes while maintaining lower R_{ct} at high voltage [70,107,109]. Further evidence comes from composite membrane systems. Likitaporn and colleagues reported that $Ti_3C_2T_x$-integrated PAN/polyurethane membranes maintained structural integrity and electrochemical stability in Zn symmetric cells, even under fast charge–discharge cycles—indicative of stable MXene behavior within the ESW in both Li and Zn battery chemistries [107]. Beyond ESW stability, MXenes play a crucial role in improving electrode–electrolyte compatibility, particularly at typically problematic interfaces like lithium anode or high-voltage cathode surfaces. Their layered, conductive structure, combined with a high-affinity surface chemistry, allows them to adhere effectively and form conformal, lithiophilic coatings that reduce interfacial resistance and extend cycle life. A recent review noted MXenes' potential to form ionically permeable and chemically benign interlayers that mitigate interfacial degradation, serving both as mechanical buffers and electron-conducting layers without generating resistive byproducts [109]. Computational and spectroscopic studies further attest to how MXenes contribute to interfacial stabilization. For example, DFT studies of MXene–Si interfaces revealed that hydroxyl-terminated Ti_3C_2 (Ti_3C_2-OH) forms significantly stronger adhesion to amorphous silicon than F-terminated variants, implicating surface chemistry in modulating interface mechanical robustness—a proxy for minimizing delamination under stress [110]. Moreover, MXene composites with oxide layers (e.g., TiO_2) show substantial interfacial electron transfer and hydrogen bonding, enhancing adhesion through specific surface terminations—an effect that can reduce charge transfer resistance at electrode–electrolyte junctions [111]. Ultimately, MXenes expand the electrochemical operation envelope of composite solid electrolytes, allowing for stable operation across elevated voltages and reactive interfaces. Their interfacial functionality, stemming from customizable terminations and layered morphology, provides both chemical passivation and mechanical compliance, enabling long-term integrity in SSBs subjected to cycling, thermal stress, or harsh chemical environments.

6. MXene-Based Interfacial Engineering in SSBs

In the relentless pursuit of high-energy-density, safe, and durable solid-state batteries (SSBs), one of the most formidable hurdles is the persistent challenge of interfacial resistance. But simply integrating high-conductivity solid electrolytes does not guarantee optimal performance, as mismatches in chemical stability, mechanical compliance, and ion transport

behavior often result in significant impedance growth during cycling. These limitations highlight the importance of interfacial engineering, where the objective is not only to facilitate efficient charge transfer across solid–solid contacts but also to stabilize the dynamic electrochemical environment in the presence of lithium dendrites, volume fluctuations, and reactive interfaces. Within this context, MXenes emerge as uniquely capable interfacial materials. Their metallic conductivity ensures continuous electron pathways, while their surface terminations and two-dimensional morphology enable strong adhesion to both solid electrolytes and electrodes. Moreover, their mechanical flexibility and ability to host functional modifications (e.g., oxide coatings, polymer grafting, or hybridization with other 2D materials) allow MXenes to buffer stresses and mitigate degradation processes. As a result, MXene-based interfacial engineering represents a multifunctional approach that directly addresses the bottlenecks of SSBs, laying the foundation for subsequent discussions on specific strategies ranging from Li^+ transport enhancement to scalable integration methods.

6.1. Interfacial Resistance Issues in SSB Architectures

In solid-state battery (SSB) architectures, the interface between electrode and electrolyte is often the Achilles' heel. Despite continuous progress in the development of solid electrolytes, such as LGPS, LLZO, or halide conductors like Li_3InCl_6, the actual performance of full cells is frequently limited by the persistent and multifactorial problem of interfacial resistance. While bulk ionic conductivities of these materials can rival or even surpass those of traditional liquid electrolytes, their integration with electrodes remains far from ideal. Factors such as poor physical contact, chemical incompatibility, and interfacial polarization collectively give rise to high-resistance regions that severely hinder charge transport and cycle life. Mechanical contact loss is among the primary sources of interfacial resistance. Solid electrodes and electrolytes tend to exhibit mismatched Young's moduli and thermal expansion coefficients, leading to void formation or delamination during cycling or temperature fluctuations. Contact loss reduces the effective area for ion transport, creating bottlenecks and current constriction points. Recent modeling and experimental work have shown that the increase in resistance with reduced contact area follows a super-linear scaling, which cannot be fully corrected by applying pressure alone due to limitations in interface compliance and material elasticity [112]. Chemical degradation also plays a significant role. At the interface, reactive combinations between electrode and electrolyte can result in the formation of unstable solid electrolyte interphases (SEIs) or cathode electrolyte interphases (CEIs) that are ionically or electronically resistive. This is particularly problematic with sulfide-based electrolytes, which are prone to redox reactions with both lithium metal and high-voltage oxide cathodes, generating decomposition products such as Li_2S, P_2S_5, or intermetallics that interrupt ion conduction pathways [113,114].

Beyond physical and chemical factors, electrostatic mismatches at the interface can induce space-charge layers or internal fields that alter ion migration behavior. These energy level discontinuities between the solid electrolyte and electrode materials lead to undesired charge accumulation and potential barriers that further suppress interfacial lithium-ion mobility. Such effects have been observed even in ostensibly stable oxide-oxide systems, indicating that electrochemical stability alone does not guarantee low interfacial resistance [115]. In this complex scenario, MXenes have emerged as highly effective materials for interfacial engineering in SSBs. Their intrinsic metallic conductivity (up to 20,000 S/cm), rich surface chemistry (e.g., -O, -OH, -F terminations), and 2D lamellar morphology enable them to fulfill multiple roles simultaneously. When applied as thin interfacial layers, MXenes conformally coat rough electrode surfaces, filling voids and smoothing contact irregularities at the nanoscale. This helps maintain intimate mechanical contact even under

dynamic conditions such as lithiation-induced volume changes or temperature cycling. Moreover, MXenes can chemically passivate unstable interfaces by physically separating incompatible materials while allowing ion transport to proceed. Their terminations can be tuned to selectively interact with specific solid electrolyte chemistries, thereby minimizing undesirable reactions and suppressing interphase formation. Additionally, recent studies have shown that MXenes can modulate local interfacial electric fields through dipole layer formation, thus lowering ion migration barriers and promoting uniform Li^+ flux across interfaces. When functionalized appropriately or embedded into polymeric matrices, they can also suppress parasitic electronic conduction pathways that would otherwise trigger electrolyte decomposition. These combined properties make MXenes uniquely suited to reduce the multifactorial resistance network at SSB interfaces, enhancing both rate performance and long-term cycling stability. A compelling example was reported by Wang et al., who employed a $Ti_3C_2T_x$-based artificial interlayer at the lithium–electrolyte interface in a solid-state Zn battery. The MXene layer maintained structural integrity, preserved chemical stability, and led to dramatic improvements in both Coulombic efficiency and impedance spectra over 500 cycles [50]. Similarly, in polymer–ceramic hybrid electrolytes, MXene-modified membranes have demonstrated superior interfacial adhesion, lower charge-transfer resistance, and improved tolerance to high current densities [107]. These findings underscore that interfacial resistance in SSBs arises from a confluence of mechanical, chemical, and electrostatic mismatches and cannot be solved by one-dimensional solutions. MXenes, through their multifunctional nature, offer an advanced platform for holistic interfacial engineering. Their use marks a shift from passive interface stabilization to active, tunable interfacial architectures that enhance ion conduction, suppress degradation, and maintain structural cohesion throughout battery operation.

6.2. MXenes as Interlayers Between Electrodes and Electrolytes

When designing solid-state batteries (SSBs), achieving robust electrode–electrolyte interfaces is pivotal—and MXene materials offer an exceptional solution as thin, multifunctional interlayers. Their flat, conductive nature and rich surface chemistries allow them to conformally coat uneven electrode surfaces, rectify contact loss, and provide persistent, ion-conductive bridges. A compelling demonstration comes from the development of a lithium–MXene composite anode tailored for garnet-type solid electrolytes, where the MXene interlayer reduced interface resistance from over 1291 $\Omega \cdot cm^2$ to just 5 $\Omega \cdot cm^2$, a dramatic improvement that stems from enhanced contact and in situ formation of LiF, which suppresses dendritic growth between Li and garnet [116]. The intrinsic interlayer spacing of Ti_3C_2 MXenes further accelerates Li^+ transport while buffering mechanical strain, acting akin to molecular "pillars" that stabilize interfacial architecture during repeated cycling. This 'pillar effect' allows for strain-free charge storage, enabling MXene-based electrodes to sustain excellent structural integrity and interface coherence under dynamic electrochemical conditions, a phenomenon directly observed via operando STEM imaging [117]. In composite electrodes combining porous silicon and MXene (PSi@C), an MXene interlayer creates conductive cross-link networks and omnidirectional Li^+ pathways, maintaining electronic continuity and minimizing charge-transfer impedance. Experimental results showed notable enhancements in both capacity retention and rate performance over comparable electrodes without MXene intervention [118]. Surface chemistry tuning of MXenes propels interfacial performance even further. For instance, nitrogen-doped MXene (N-MXene) layers placed adjacent to silicon anodes create preferential Li^+ transport routes and dramatically reduced interfacial resistance, significantly boosting high-rate capacity and cycle life for alloying anode systems [119]. In high-voltage sulfide–oxide interfaces, MXene interlayers undergo in situ transformation into lithium titanate (Li_2TiO_3),

forming a stable chemical buffer that mitigates detrimental redox reactions and extends the operational window to ~4.5 V while preserving ionic conductivity, cycling stability, and rate capability [120].

Beyond material chemistry, MXenes enhance interfacial adhesion. DFT analyses of MXene–TiO_2 heterostructures reveal that -OH-terminated MXene forms nearly 0.9 electrons per nm^2 of charge transfer to TiO_2, fostering strong hydrogen-bond-reinforced adhesion and exceptional electronic overlap—key for stabilizing mechanically sensitive interfaces [111]. Related modeling of Si–MXene interfaces shows that fully hydroxylated Ti_3C_2 MXene exhibits significantly higher interface strength (0.6 J/m^2) with amorphous silicon than oxygen- or fluorine-terminated variants, highlighting how surface functionalization tailoring can optimize mechanical resilience and Li^+ adhesion [110]. Even under harsh operating conditions, MXene interlayers retain their functional performance. For instance, advancements in separator engineering using MXene coatings improve electrolyte wettability and mechanical integration without sacrificing ionic conductivity or long-term stability [121]. These qualities reinforce MXene's appeal for scalable, durable SSB production.

6.3. Chemical Compatibility and Suppression of Interfacial Reactions

Even under optimal contact conditions, chemical incompatibility at electrode–electrolyte interfaces poses a persistent threat to solid-state battery (SSB) performance. Specifically, sulfide electrolytes—widely appreciated for their high ionic conductivity—commonly undergo reductive breakdown in contact with lithium metal or oxidative degradation at high-voltage cathodes, generating resistive interphases and elevating impedance. Ren et al. thoroughly explore these issues, identifying both the root causes and potential strategies to suppress harmful interfacial reactions, including buffer layers and surface coatings [122]. MXene interlayers offer multiple safeguards against such degradation pathways. First, they act as chemically inert buffer layers. When a $Ti_3C_2T_x$ MXene is placed between lithium and a garnet-type solid electrolyte, it consistently fosters the in situ formation of a thin LiF-rich interphase. This self-generated layer substantially retards electronic leakage and dendrite penetration, leading to extraordinarily low interfacial resistance and enabling a critical current density up to 1.5 mA/cm^2 [116]. MXenes also exhibit inherent chemical stability toward both lithium and high-voltage oxides, further preventing destructive interphases. Wang et al. demonstrated that MXene-bonded conductive networks embedded in polymer electrolytes maintain interface integrity across full cycling in solid-state Zn batteries, without succumbing to parasitic interfacial reactions [50]. Under oxidative potentials, sulfide SSEs interfacing layered oxide cathodes (LCO/NMC) tend to form resistive CEI species; MXene-based cathode interlayers or MXene@oxide hybrids act as electron-percolating yet chemically tempering films that (i) limit sulfide oxidation, (ii) reduce interfacial OER-like parasitics, and (iii) preserve short Li^+ pathways in thick electrodes. In oxide and halide SSEs, the priority is contact and adhesion: MXene lamination of cathode/SSE surfaces spreads the electric field and minimizes local potential gradients, sustaining low interfacial resistance at 4.3–4.5 V [109,120].

On a molecular level, surface-engineered MXenes (e.g., -OH terminated) can establish strong, hydrogen-bonded interfaces with oxide-based materials. Xu et al. used first-principles calculations to show that there is ~0.9 electrons/nm^2 of interfacial electron transfer from OH-terminated MXene to TiO_2, with robust adhesion as a result of both charge transfer and hydrogen bonding, underscoring how MXenes chemically stabilize interfaces [111]. Furthermore, the ionic affinities of MXene surfaces help anchor reactive species, suppressing their migration and chemical degradation. In the context of lithium–selenium batteries, DFT studies reveal that S- and O-terminated Ti_3C_2 MXenes bind strongly to intermediate polyselenides like Li_2Se_n, anchoring them and preventing shuttle effects

that otherwise lead to capacity loss—while preserving their own conductivity [123]. These functionalities collectively stabilize electrode–electrolyte interfaces across multiple dimensions: mechanically, chemically, and electronically. MXenes, through a blend of passive buffering, selective chemical interaction, and conductive passivation, suppress harmful interfacial chemistry, unlike traditional interfacial coatings that can degrade or delaminate over time.

6.4. Integration Strategies for Scalable Fabrication

Developing reliable and scalable manufacturing techniques for MXene interlayers in solid-state batteries (SSBs) is pivotal for translating lab-scale innovations into real-world applications. Techniques such as roll-to-roll processing, solution-based deposition, template engineering, and vapor-phase fabrication enable controlled, area-scalable MXene integration—each with tradeoffs in film quality, throughput, and interfacial functionality. Solution-processable MXene inks form the backbone of many scalable interfacial deposition strategies. MXenes disperse effectively in aqueous or polar organic solvents such as water, ethanol, DMF, and propylene carbonate, facilitating uniform deposition through methods like spin coating, spray coating, dip coating, vacuum filtration, and roll casting. This versatility supports conformal film formation across electrodes and electrolytes with complex topology, while achieving controlled thickness and coverage [124]. Blade coating, in particular, has emerged as a practical method for producing uniform MXene interlayers on a large scale. In a recent study, Guo et al. demonstrated that blade-coated $Ti_3C_2T_x$ films exhibit consistent electrical properties and environmental stability over extended periods, which is vital for practical SSB manufacturing workflows [125]. The ability to control coating thickness down to nanometer precision enables the fine-tuning of interfacial resistance and ionic accessibility. Other innovative approaches include the formation of liquid crystalline MXene phases, which promote alignment of 2D flakes during deposition. Yuk et al. developed biologically inspired "surface-bridging" structures that self-organize into aligned films with enhanced conductivity and mechanical resilience, offering promise for scalable fabrication of MXene-based separators and interlayers [126]. In multi-layered electrode systems or composite solid-state architectures, vacuum-assisted filtration (VAF) has been used to create densely packed MXene films with tunable porosity and high adhesion to polymeric and inorganic substrates. This method is particularly attractive when high areal loading and minimal solvent residue are required [124]. On the chemical vapor deposition (CVD) front, emerging studies have begun to explore vapor-phase synthesis routes for MXenes, particularly for carbide or nitride variants that may bypass hazardous etching processes. While these techniques currently lack the throughput of wet methods, they enable high crystallinity, precise control over stoichiometry, and exceptional compatibility with microfabrication workflows [127].

One of the main obstacles during the scale-up of MXene-based films is their strong tendency to restack, which reduces interlayer spacing and severely limits Li^+ transport. To mitigate this problem, several approaches have been proposed, including the introduction of molecular or ionic pillars (e.g., CTAB, Sn^{4+}) and the pre-intercalation of species such as Li^+ or DMSO, which help to preserve interlayer galleries and maintain porosity during film processing. A particularly effective solution has been reported by Abdolhosseinzadeh et al., who designed porous $Ti_3C_2T_x$ films with tunable density using a urea-assisted, template-based strategy. Removal of the template yielded interconnected pores that prevented dense restacking, facilitated ion diffusion, and improved mechanical integrity. These porous architectures demonstrated excellent electrochemical performance and robustness, both of which are critical for solid-state integration [128]. Figure 4 illustrates this approach, showing SEM cross-sections of MXene films with varying densities, photographs and surface views

of pristine and porous samples, as well as profilometry and nitrogen adsorption data confirming the increased porosity and surface area after template removal [128]. MXene interlayers have also demonstrated remarkable long-term storage stability under ambient conditions. In a recent study, Lee et al. reported that $Ti_3C_2T_x$ films stored for up to 5–9 years in sealed environments retained over 90% of their conductivity, making them well-suited for incorporation into production chains where shelf life and robustness are vital [108].

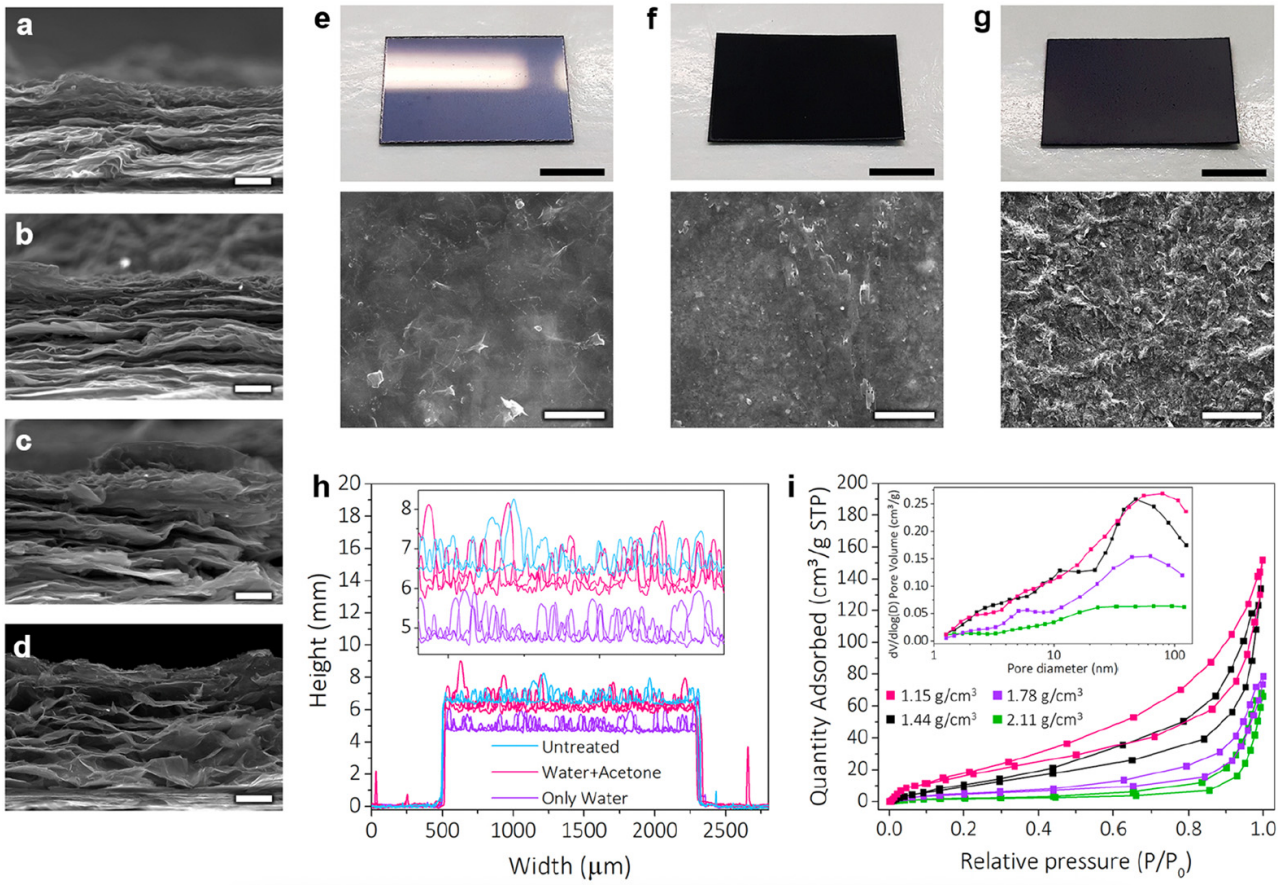

Figure 4. Cross-sectional SEM images of MXene films with progressively reduced densities: pristine (2.11 g cm^{-3}) (**a**), 1.78 g cm^{-3} (**b**), 1.44 g cm^{-3} (**c**), and 1.15 g cm^{-3} (**d**). All micrographs use a 2 μm scale bar. Panels (**e**–**g**) display photographs (top, scale bar: 2 cm) and surface SEM views (bottom, scale bar: 30 μm) of the pristine film, the MXene-urea composite, and the porous MXene obtained after urea removal, respectively. Profilometry measurements of film thickness for samples treated with water, water/acetone, and untreated controls, confirming increased porosity after urea dissolution (**h**). Nitrogen adsorption–desorption isotherms of films with different densities, showing a direct correlation between reduced density and higher specific surface area (95.6 m^2 g^{-1} for 1.15 g cm^{-3}, down to 10.5 m^2 g^{-1} for 2.11 g cm^{-3}) (**i**). (Adapted with permission from ref. [128], Chemistry Europe 2021).

Taken together, these scalable integration methods—ranging from solution-based deposition to vapor-phase growth and alignment strategies—enable the deployment of MXene interlayers across large-format SSB components with exceptional control over thickness, adhesion, ionic pathways, and chemical functionality. Overcoming technical obstacles such as sheet aggregation, oxidation, and interfacial delamination through smart processing design is critical to the commercial realization of MXene-enabled SSBs.

7. Challenges and Limitations

Despite the remarkable multifunctionality and versatility of MXenes in solid-state batteries (SSBs), their practical deployment at the industrial scale remains far from trivial. While laboratory-scale studies have demonstrated impressive electrochemical performance, enhanced interfacial compatibility, and improved mechanical resilience, several critical challenges hinder the transition from proof-of-concept to manufacturable, commercially viable systems. These limitations are multifaceted, encompassing materials chemistry, environmental safety, engineering integration, and economic feasibility. The complexity of MXene synthesis, the instability of their surface chemistry under ambient conditions, and the intrinsic cost associated with both raw precursors and downstream processing all contribute to a performance-scalability gap. Furthermore, while most reports focus on short-term cycling and idealized cell architectures, far less attention has been devoted to the long-term chemical stability, environmental footprint, and compatibility of MXene-enabled systems with existing battery manufacturing infrastructure.

This section outlines the major bottlenecks that currently limit the large-scale application of MXenes in SSBs. It is structured into three subsections: (i) synthesis scalability and environmental concerns, (ii) chemical stability and oxidation resistance, and (iii) cost and integration barriers in manufacturing. Together, these challenges represent the "non-electrochemical" dimension of MXene research—factors that will ultimately determine whether these materials can bridge the gap between laboratory discovery and industrial reality.

7.1. Material Synthesis Scalability and Environmental Concerns

The majority of MXene-based studies to date rely on small-batch synthesis routes, typically involving either hazardous etching chemistries (e.g., concentrated HF or in situ HF from LiF/HCl mixtures) or energy-intensive molten-salt processes. While these approaches yield high-quality materials suitable for academic investigation, they pose significant barriers to large-scale manufacturing from both a safety and sustainability perspective.

7.1.1. Limitations of Conventional Wet-Etching Routes

The earliest and most widely used synthesis method for MXenes remains direct HF etching of MAX phases, as introduced by Naguib et al. [10]. Although HF etching produces highly crystalline, delaminated $Ti_3C_2T_x$ with good yield and reproducibility, the use of concentrated HF (typically 40–50 wt %) raises serious occupational and environmental hazards. HF is acutely toxic, highly corrosive, and requires dedicated infrastructure for handling, neutralization, and waste treatment. Scaling this chemistry to kilogram or ton-scale production introduces disproportionate risks and costs. In response to these concerns, in situ HF generation methods using LiF + HCl or NaF + HCl have become popular alternatives. These routes are milder, safer to handle, and allow simultaneous Li^+ intercalation, which facilitates delamination and increases interlayer spacing [36]. However, the environmental footprint remains non-negligible. Recent life-cycle assessments (LCA) by revealed that LiF/HCl-based etching still involves significant fluoride waste generation and requires substantial water and energy input for neutralization and purification [129]. Moreover, these aqueous etching methods are inherently batch-limited: the reaction kinetics are slow (typically 12–48 h), yield large volumes of acidic effluent, and are difficult to continuously scale due to non-linear delamination behavior. As a result, industrial adoption would require expensive modular reactors or continuous-flow systems with in-line neutralization—technologies that are still in early development stages [35].

7.1.2. Challenges of Molten-Salt and Fluorine-Free Synthesis

Molten-salt etching (e.g., $ZnCl_2$, $CuCl_2$, $FeCl_3$) has emerged as a promising HF-free alternative capable of producing Cl-terminated MXenes with enhanced environmental stability [130]. These reactions occur at elevated temperatures (500–700 °C) and avoid the use of liquid acids altogether. Nevertheless, molten-salt methods face several scalability challenges:

- Energy intensity: High-temperature operation results in elevated energy costs and requires corrosion-resistant reactors.
- Post-processing complexity: Residual salts must be thoroughly removed via extensive washing or vacuum annealing, generating additional wastewater and prolonging processing time.
- Control over stoichiometry: Non-uniform etching or incomplete removal of A-layer elements can produce MXenes with heterogeneous surface chemistry and mixed phases, which impairs reproducibility [131].

Fully fluorine-free hydrothermal methods using NaOH or KOH are attractive from a green chemistry standpoint but remain largely limited to Ti-based MAX phases and suffer from incomplete etching or oxide contamination [38].

7.1.3. Raw Material and Precursor Considerations

Another factor affecting scalability is the availability and cost of MAX phase precursors. High-purity Ti_3AlC_2 or Nb_2AlC powders are typically synthesized via high-temperature solid-state reactions (1300–1500 °C) from metallic powders and carbon sources. These processes are energy-intensive and require careful stoichiometric control to avoid secondary phases. MAX phase synthesis represents >40% of the total energy footprint of MXene production [129]. Furthermore, the cost of transition metals such as Nb, V, or Mo can significantly impact the price per gram of specialty MXenes.

7.1.4. Environmental Impact and Sustainability

From an environmental perspective, the main sustainability concerns include:

- Fluoride waste management: Effluents containing LiF, AlF_3, and other fluorides require specialized neutralization and disposal.
- Water consumption: Washing and delamination steps consume large quantities of deionized water, with up to 50–100 L of rinse water per gram of MXene reported in some protocols [129].
- Energy footprint: Both MAX phase synthesis and post-etching treatments (e.g., freeze-drying, annealing) are energy-intensive, raising concerns about the net carbon footprint of MXene production.

A recent comparative LCA concluded that the global warming potential (GWP) of conventional $Ti_3C_2T_x$ synthesis is approximately 75–100 kg CO_2-eq per kg of product, substantially higher than that of carbon black or graphene oxide, and far exceeding the sustainability benchmarks for battery-grade materials [132].

7.1.5. Pathways Toward Scalable and Sustainable Synthesis

To address these barriers, several strategies are being actively explored:

- Continuous-flow microreactors for LiF/HCl etching have been demonstrated to reduce batch time and improve yield consistency, as reported by Kim et al. [133].
- Molten-salt recycling and closed-loop HF recovery systems have been proposed to reduce chemical waste and improve sustainability metrics [134].

- Low-temperature plasma etching and mechanochemical exfoliation are emerging as dry alternatives that bypass liquid etching entirely, although scalability and termination control remain under investigation [135].
- Green chemistry frameworks integrating solvent recovery, fluoride capture, and water reuse are essential to reduce the overall environmental impact and cost.

In summary, while MXenes offer unmatched multifunctionality for SSB architectures, their current synthesis methods present significant obstacles to large-scale, environmentally responsible production. Overcoming these challenges will require coordinated innovation across materials chemistry, chemical engineering, and sustainability science.

7.2. Chemical Stability and Oxidation Resistance of MXenes

The usefulness of MXenes in solid-state batteries ultimately hinges on preserving their high electronic conductivity and interfacial functionality under processing and operating conditions that are often dry, moderately hot, and oxygen-exposed. Oxidation is the dominant degradation pathway for Ti-based MXenes (e.g., $Ti_3C_2T_x$), proceeding via nucleation and growth of TiO_2 at edges and defect sites, accompanied by loss of metallic conductivity and structural delamination. Recent mechanistic work has clarified that confined water, that is, water trapped between layers and at surface terminations, plays a catalytic role in initiating and accelerating this transformation, even when films are nominally "dry." Removal of confined water prior to air exposure substantially slows oxide formation, directly linking hygroscopicity to ambient degradation kinetics and offering a practical handle for stabilization during SSB fabrication steps [136]. Beyond moisture, the storage medium and physical state strongly modulate oxidation rates. A multi-media study showed that $Ti_3C_2T_x$ oxidizes fastest in aqueous dispersions, more slowly in organic solvents, and slowest in solid films and polymer composites, yet color or colloidal appearance can remain deceptively unchanged while conductivity plummets, underlining the need for quantitative monitoring during materials handling. These observations rationalize why aqueous inks that are convenient for coating electrodes or interlayers can be counterproductive unless oxygen is excluded or chemical scavengers are present. In practice, deoxygenated, low-temperature handling and fast drying are essential whenever wet steps are unavoidable [137].

Chemical mitigation strategies that are compatible with battery-grade processing have emerged. Antioxidants such as sodium L-ascorbate effectively suppress oxidation in aqueous colloids for extended periods by scavenging dissolved oxygen and reactive intermediates, enabling formulation, transport, and deposition of MXene inks with far less degradation. While such additives are typically removed or minimized before final cell assembly, the underlying principle, quenching solution-phase oxidants to preserve surface terminations, provides a generalizable route to maintain MXene integrity through wet steps that precede SSB dry-room integration [138].

Long-term and thermal stressors relevant to SSB manufacturing introduce additional constraints. In ambient storage spanning years, free-standing $Ti_3C_2T_x$ films exhibit conductivity loss largely attributable to water uptake rather than irreversible lattice collapse; importantly, vacuum annealing can restore much of the conductivity by desorbing moisture. This result suggests that some "aging" labeled as oxidation in the literature is, in practice, a reversible hydration effect, with obvious implications for warehouse storage, electrode preconditioning, and hot-press steps. Nonetheless, once crystalline TiO_2 forms, conductivity losses are not recoverable, emphasizing the importance of keeping both water activity and oxygen partial pressure low throughout the processing window [108].

At elevated temperatures, oxidation accelerates; however, materials design can extend the usable thermal window. Composite architectures that physically and chemically hinder

oxygen access to MXene surfaces have achieved remarkable high-temperature stability in air (>400 °C) without catastrophic loss of function, pointing to barrier-layer and encapsulation strategies that may be adapted to SSB interlayers which experience thermal excursions during drying, calendaring, or lamination. From a practical standpoint, this means that thin, conformal barriers deposited prior to heat treatment can be worth the added processing complexity if they preserve MXene conductivity through the thermal budget of SSB electrode and electrolyte consolidation [139].

Surface chemistry also controls intrinsic stability. Theory and experiment indicate that the identity and coverage of terminations (-O/-OH/-F vs. halide or chalcogen species) determine adsorption energetics for O_2/H_2O and, by extension, oxidation susceptibility. Halogen-terminated MXenes prepared in Lewis-acid molten salts (e.g., $Ti_3C_2Cl_2$) have been obtained with high termination purity and show altered oxidation behavior relative to conventional aqueous-etched $Ti_3C_2T_x$, providing a complementary route to stability via synthetic control of surface chemistry rather than only post-processing protection. For SSBs, where polar polymer or oxide electrolytes contact MXene interlayers, tuning terminations to balance stability with interfacial ion transport (and avoiding hydrolyzable groups) is a rational design axis [140,141].

Finally, robust process recommendations emerge from this body of evidence: minimize residence time in water and oxygenated solvents; use deoxygenated media and antioxidants during unavoidable wet processing but remove residues before cell closure; prefer film-first or dry-transfer routes; store powders/films under dry inert gas or vacuum and, when needed, restore conductivity by brief vacuum anneals; design barrier architectures (e.g., ultrathin Metal–Organic Framework or MOF, or oxide passivation layers) that limit O_2/H_2O ingress during heating; and, when compatible with the target electrolyte, leverage termination engineering (including molten-salt approaches) to intrinsically slow oxidation while maintaining electronic percolation at the interface. Together, these measures have already enabled real gains: slower ambient degradation, preserved conductivity during processing, and greater tolerance to thermal steps typical of SSB manufacturing, all prerequisites for translating MXene-enabled interfaces from lab-scale prototypes to durable, manufacturable SSB stacks [142–144].

7.3. Cost and Integration Barriers in SSB Manufacturing

While MXenes offer remarkable multifunctionality in solid-state batteries (SSBs), serving as conductive additives, protective interlayers, and structural reinforcements, their transition from laboratory demonstrations to industrial-scale production is constrained not only by synthesis and stability challenges but also by economic and manufacturing integration barriers. The scalability of MXene technologies requires balancing performance benefits with practical considerations such as cost of raw materials, process throughput, compatibility with established battery fabrication lines, and long-term reliability.

One of the foremost barriers lies in the economic cost of MXene synthesis. High-purity MAX precursors such as Ti_3AlC_2 or Nb_2AlC typically require high-temperature solid-state reactions (above 1400 °C) and high-purity metallic precursors, leading to energy-intensive and expensive production steps. For Ti-based MXenes, the use of hydrofluoric acid (HF) or LiF/HCl etching routes further increases costs due to the need for specialized facilities, acid handling protocols, and waste treatment systems. Recent techno-economic analyses of MXene synthesis suggest that the cradle-to-gate production cost of $Ti_3C_2T_x$ can exceed USD 200–400 per kilogram at laboratory scale, largely due to precursor synthesis and chemical consumption [145]. Although this figure may decline with scale-up and process optimization, it still compares unfavorably with the cost of carbon additives such as Super P (<USD 20 per kilogram) or conventional ceramic fillers [146]. Another major challenge is

the integration of MXenes into SSB manufacturing lines, which are themselves evolving from liquid electrolyte processing to dry or solvent-assisted routes. Traditional slurry coating processes in lithium-ion battery production are optimized for carbon black or graphene-based conductive agents dispersed in N-methyl-2-pyrrolidone (NMP) or water-based systems. MXenes, although dispersible in aqueous or polar solvents, are highly sensitive to oxygen and moisture, making their use in existing electrode fabrication facilities difficult without significant adaptation. Advanced strategies, such as roll-to-roll vacuum-assisted filtration or spray deposition of deoxygenated MXene inks, have been proposed for scalable electrode and separator coatings, but these require substantial capital investment in inert-gas handling systems and solvent recycling units [125,147,148]. In addition, the restacking tendency of MXene nanosheets during drying or calendaring leads to performance variability and non-uniform interfaces when scaling to large-format electrodes. Overcoming this requires the introduction of spacers (e.g., polymers, metal cations, or small organic molecules) to maintain interlayer distances, but such modifications add processing steps and may increase costs. Similarly, the integration of MXenes with brittle ceramic electrolytes demands controlled lamination pressures and sometimes interfacial adhesives or secondary buffer layers, which complicates the manufacturing sequence and may reduce throughput. From a supply-chain perspective, the limited number of large-scale MXene producers and the reliance on specific MAX phase precursors (often requiring vanadium, niobium, or molybdenum) raise questions about resource availability and price volatility. For example, the global production of Nb_2O_5, a key raw material for Nb-based MXenes, is geographically concentrated, which introduces potential risks of supply disruption [149]. Furthermore, while Ti-based MXenes are relatively abundant, achieving consistent high-quality batches with controlled terminations remains non-trivial, necessitating stringent quality assurance measures that increase overall cost. Environmental compliance also intersects with manufacturing feasibility. Large-volume fluoride-containing effluents from HF or in situ etching require energy-intensive neutralization and disposal, which can significantly raise operating expenditures and pose regulatory barriers, particularly under the European Union's REACH framework or U.S. Environmental Protection Agency (EPA) guidelines [69,150,151]. In this context, greener etching methods, including fluoride-free hydrothermal processes and molten-salt routes with recycling schemes, are gaining attention as potential pathways to improve environmental sustainability and lower long-term costs [38].

Ultimately, the successful deployment of MXenes in SSB manufacturing will depend on process integration with existing gigafactory infrastructure. Approaches that enable scalable deposition (such as slot-die or blade coating of MXene-based slurries), restacking mitigation through rational interlayer engineering, and closed-loop chemical management will be crucial. Recent work has shown that hybrid deposition strategies combining MXenes with polymer matrices can be adapted to roll-to-roll processes, offering a feasible transition route from laboratory demonstrations to industrial production [147]. Nevertheless, the economic gap between laboratory-scale MXenes and conventional carbon-based additives remains a significant obstacle. Without substantial advances in precursor synthesis efficiency, waste minimization, and supply-chain development, the cost of MXene-enabled SSBs is likely to remain prohibitive for widespread commercial deployment.

8. Future Perspectives

Although MXene-based solid-state batteries (SSBs) have made significant progress in recent years, several scientific and technological hurdles remain before they can be fully implemented in commercial devices. Current research has demonstrated that MXenes offer exceptional electrical conductivity, mechanical robustness, and surface tunability, all of

which are valuable for improving electrode–electrolyte interfaces and enabling high-rate capabilities. However, challenges such as material cost, large-scale manufacturing, environmental stability, and compatibility with both polymeric and inorganic solid electrolytes still limit their deployment in practical systems. Future efforts must focus on designing engineered MXene heterostructures and hybrid materials that can synergistically combine the advantages of MXenes with other functional phases (e.g., polymers, metal oxides, metal–organic frameworks). By tailoring surface chemistry, layer spacing, and composite architectures, it is possible to enhance ionic transport, suppress dendrite formation, and achieve long-term electrochemical stability under operating conditions. These directions, detailed below, represent crucial opportunities for advancing MXene-based SSBs from laboratory demonstrations toward scalable, commercial energy storage solutions.

8.1. Design of MXene Heterostructures and Hybrids for SSBs

The next performance jump for MXene-enabled solid-state batteries (SSBs) will likely come from heterostructures and hybrids that decouple electronic and ionic transport, suppress interfacial degradation, and preserve microstructural integrity under manufacturing and cycling stresses. Pristine $Ti_3C_2T_x$ offers outstanding metallic conductivity but is susceptible to restacking and ambient oxidation, both of which raise interfacial resistance and diminish long-term stability; systematic studies show oxidation proceeds fastest in liquid media and slowest in solids, while antioxidant additives can markedly retard degradation during processing, a practical consideration when formulating inks for scalable coatings [137,138]. A first design axis is MXene-polymer/MOF composites that convert 2D sheets into mixed ion-electron scaffolds with mechanical compliance. In polymer electrolytes, MXene-based hybrids can raise salt dissociation and create percolative ion-transport pathways when surface terminations are judiciously controlled and restacking is mitigated. For example, ZIF-8@MXene reinforced polymer electrolytes reached ~4.4 mS cm^{-1} ionic conductivity and a Li^+ transference number ≈ 0.76, while also improving tensile strength and flame retardancy, attributes directly relevant to safe, thin solid electrolytes. Earlier reviews established that MXenes are particularly efficient nanofillers in composite polymer electrolytes compared with 0D/1D additives, clarifying the mechanistic basis for these gains [53,152]. A complementary direction is multi-phase hybrids that bridge polymer and inorganic SSEs. Recent work combining $Ti_3C_2T_x$/PAN nanofibers with Lithium Lanthanum Zirconium Tantalum Oxide (LLZTO) particles inside a PEO matrix produced solid electrolytes with improved ionic transport and interface quality to Li metal, exemplifying how an MXene sub-network can couple mechanically compliant polymers to fast-ion ceramic fillers—an architecture that is particularly attractive for SSB stacks where oxide SSEs are laminated to Li or to high-loading cathodes [153]. Because heterostructure performance is inseparable from surface chemistry, a second design axis is termination engineering using Lewis-acid molten-salt (LAMS) routes that yield Cl-terminated MXenes (e.g., $Ti_3C_2Cl_2$) with more uniform termination populations and altered environmental reactivity relative to aqueous-etched $Ti_3C_2T_x$. Critically, new delamination protocols for LAMS-MXenes preserve their halide termination, enabling solution processing without reverting to HF chemistry; comprehensive reviews now frame these LAMS approaches as scalable, HF-free pathways that can better align with dry-room SSB manufacturing [39,130]. Mechanical robustness at scale is the third lever. Bridging-induced densification produces compact, strong MXene membranes with high conductivity and toughness, suitable as ultra-thin current-collectors or interfacial "shock absorbers" between rigid ceramic SSEs and active layers—useful wherever lamination, calendaring, or thermal steps would otherwise fracture a brittle interface. At the same time, ink design for blade/slot-die coating of MXene films provides a practical route to integrate these layers into roll-to-roll lines,

easing translation from lab coupons to large-area electrodes and interlayers [125,148]. Putting these threads together, a target MXene heterostructure for SSBs might combine (i) a LAMS-derived, oxidation-resistant MXene film that maintains electronic percolation; (ii) a MOF-decorated or polymer-tethered interface that furnishes Lewis-acid sites and ordered nanochannels for Li^+; and (iii) a densified MXene sub-layer that equalizes current and absorbs mechanical mismatch with oxide or sulfide SSEs. Reporting standards should emphasize interfacial resistance and its stability (R_{int} vs. time/temperature), CCD, Li^+ transference number, and tortuosity-normalized effective ionic conductivity in full solid-state stacks, not only in half-cell surrogates. Given the maturing toolset—antioxidant processing to preserve flakes, LAMS chemistry for termination control, densification for mechanics, and printable inks for scale—the design space for MXene hybrids is now concrete enough to support gigafactory-compatible SSB prototypes [130,138,148].

8.2. Theoretical Insights and Computational Studies Guiding Material Optimization

Computational modeling and theoretical studies play an increasingly influential role in guiding the rational design of MXene-based materials for solid-state batteries (SSBs). Across scales, ranging from first-principles DFT to continuum-level simulations, these methodologies help us understand ionic transport mechanisms, surface chemistry effects, and interfacial stability. At the atomic scale, first-principles investigations have been invaluable in identifying promising MXene compositions and terminations for ion storage and transport. A comprehensive review highlighted how theoretical screening enables rapid exploration of the vast MXene compositional space and predicts which structures offer high lithium-ion capacity, favorable adsorption sites, and optimal redox potentials for electrode applications [154]. Another key study examining mixed termination effects (-O, -F, -OH) showed that structural simplifications used in many models can still approximate real behavior surprisingly well, explaining deviations between theoretical predictions and experimental performance [155]. Theoretical analyses of surface terminations also highlight their role in tuning ion insertion energetics. Computational work has shown that O- or F-terminated Ti_3C_2 and V_2C MXenes can significantly reduce Li^+ diffusion barriers—down to ~0.22 eV in certain Mo_2TiC_2/MoS_2 heterostructures—which is promising for accelerating charge–discharge rates [156,157]. Moreover, DFT-guided design of MXene-MoS_2 heterostructures demonstrated synergistic effects: oxygen-terminated surfaces not only lowered diffusion barriers but also stabilized the interface, addressing one of the main bottlenecks in solid-state batteries [158]. Beyond monolayer transport phenomena, theoretical modeling informs the behavior of MXene hybrids and heterostructures. For instance, calculations on $Ti_3C_2T_x$ combined with 1T-MoS_2 revealed that oxygen- or fluorine-terminated MXenes significantly lower lithium ion diffusion barriers—down from ~0.80 eV to as low as ~0.22 eV—and increase diffusion coefficients by multiple orders of magnitude, directly indicating the importance of surface functionalization in accelerating ion transport in SSB interfaces [159]. Complementary to atomistic modeling, multiscale simulations have begun to quantify how MXene-based architectures perform at the device level. An exemplary case is a solid polymer electrolyte (SPE) reinforced with surface-engineered MXenes, where DFT, COMSOL simulations, and experimental data were combined to demonstrate stable lithium plating/stripping for over 2100 h, ionic conductivity of ~1.49×10^{-4} S/cm at 30 °C, and a Li-ion transference number of approximately 0.59—illustrating how theory and experiment can reinforce each other to validate material designs [160]. Overall, theoretical and computational work is shaping three principal directions:

- High-throughput compositional discovery, enabling the identification of MXene stoichiometries and terminations with advantageous ion transport, redox, and stability profiles.

- Interface modeling and hybrid architecture optimization, quantifying the roles of termination, heterostructure design, and ion conduction pathways in interfacial layers and solid electrolytes.
- Multiphysics validation, combining DFT with continuum methods (e.g., finite element or phase-field models) to evaluate macroscale stability, throughput potential, and manufacturability.

Together, these approaches form a robust roadmap for optimizing MXene materials—not by trial and error, but through targeted computational design—paving a faster, more predictable path from theory to experimental validation to scalable SSB integration.

8.3. Emerging MXene Compositions (e.g., Double Transition Metal MXenes)

The MXene family continues to expand through the design of double transition metal (DTM) compositions—in which two distinct transition metals occupy the M-sites within the lattice. This innovation broadens the compositional space beyond monometallic MXenes, facilitating fine-tuning of electronic, magnetic, and electrochemical properties [161]. Within this class, researchers distinguish between ordered structures such as $M'_2M''C_2$ or $M'_2M''_2C_3$ and solid solutions, both of which enable improved conductivity, versatile surface terminations, and enhanced chemical stability [161,162]. First-principles computational studies, particularly those using DFT, have been pivotal for guiding this optimization. Screening of thousands of candidate DTM MAX phases has identified materials with favorable formation energies, high Li-ion capacities, and low diffusion barriers, many of which are cataloged in open-access databases such as nanoHUB's MXene dataset [157]. For example, Mo_2TiC_2 and $Mo_2Ti_2C_3$ have been predicted and experimentally realized, showing high electrical conductivity and large interlayer spacing beneficial for fast ion transport [156,162]. Beyond electrochemical performance, mechanical robustness and processability are also critical. Recent work on bridging-induced densification of $Ti_3C_2T_x$ films revealed that strong interflake interactions can yield high strength and flexibility without sacrificing conductivity, a desirable trait for solid-state battery integration [156]. Overall, emerging DTM MXenes and engineered heterostructures represent a powerful design frontier. By leveraging computational insights, high-throughput materials databases, and advances in scalable synthesis, researchers are developing MXenes with tailored properties for high-energy, long-cycle-life solid-state batteries. At the same time, ensuring compliance with regulatory frameworks for nanomaterials will be essential to transition these innovations from laboratory prototypes to industrial deployment [158,161].

8.4. Integration with Emerging Solid Electrolytes (e.g., Sulfide, Halide-Based)

Integrating MXenes with next-generation solid electrolytes—such as sulfide- and halide-based systems—offers a compelling pathway to address the interfacial compatibility challenges in solid-state batteries (SSBs). Sulfide electrolytes like argyrodites (e.g., Li_6PS_5Cl) and oxide analogs have exceptional ionic conductivity (>1 mS/cm) but often suffer from poor interfacial stability and moisture sensitivity. MXenes, with their metallic conductivity and tunable surface chemistry, can act as interfacial buffers, preserving electrochemical performance and mechanical integrity. Recent research demonstrates that $Ti_3C_2T_x$ MXenes maintain strain-free charge storage behavior when paired with inorganic solid electrolytes, preserving interfacial contact even during repeated Li^+ (de)intercalation. Operando STEM-EELS studies revealed a "pillar effect" from trapped Li^+ in MXene interlayers, enabling long-term stability in full SSB architectures [117]. Beyond this, MXene-containing interlayers (for example, incorporating graphene oxide, carbon nanotubes, and MXene) have been embedded in LATP ($Li_{1.3}Al_{0.3}Ti_{1.7}(PO_4)_3$) solid electrolytes via thermal pulse sintering. These hybrid interfaces significantly reduce impedance and improve cycle

stability at high voltages (e.g., with $LiCoO_2$ cathodes) [109]. Another emerging strategy combines MXenes with composite sulfide/polymer electrolytes to survive ambient processing conditions. For instance, modifying sulfide electrolyte surfaces with hydrophobic thiols extends their resistance to moisture and allows stable handling in humid environments, while preserving ionic conductivity for >2 days [163]. Such surface engineering techniques are crucial when designing MXene-integrated SSBs using sulfide electrolytes. At a more fundamental level, DFT and spectroscopic studies are revealing the degradation mechanisms of sulfide electrolytes at the atomic scale, such as PS_4 tetrahedron distortion and S-S bond formation during delithiation, which increases interfacial resistance. Insights from these studies help clarify how MXene interlayers could mitigate such degradation by offering electronically conductive, conformal contact layers [164]. Taken together, MXenes represent a versatile toolkit for enhancing the interface with advanced solid electrolytes. Whether through strain-tolerant interlayers, conductive hybrid coatings, or surface-protector functionalization for processing resilience, MXenes hold significant promise for unlocking the full capabilities of sulfide- and halide-based SSBs.

8.5. Roadmap Towards Commercial Implementation

Bringing MXenes into the commercial realm of solid-state batteries (SSBs) requires a multi-stage roadmap that bridges laboratory innovation with scalable, safe, and economically viable production. A foundational milestone is achieving scalable, low-cost, and environmentally responsible synthesis methods. As highlighted by Gogotsi, transitioning away from hazardous HF-based etching toward greener, greener, and scalable techniques—such as molten-salt or electrochemical routes—is essential for industrial viability [165]. Simultaneously, techno-economic analyses identifying energy costs, waste management infrastructure, and cost projections across production scales are urgently needed. Mim et al. provided a comprehensive lifecycle evaluation that ties lab-scale performance with process economics and outlines strategic investment points where cost-saving and sustainability intersect [166]. Parallel to synthesis advancement is establishing reliable interface engineering protocols. The UCSD-led commercialization roadmap for all-solid-state batteries prioritizes stable electrode–electrolyte interfaces, standardized in operando characterization methods, scalable cell architectures, and recyclability by design [167]. MXenes themselves offer a unique advantage here: their metallic conductivity, tunable termination chemistry, and mechanical flexibility make them strong candidates for interfacial coatings or current collectors that preserve contact and reduce resistance, but only if reproducible manufacturing procedures are developed. The third critical pillar is building manufacturing processes compatible with gigafactory production. Techniques such as slot-die or blade coating of MXene inks, roll-to-roll densification, and flexible current collector integration must be scaled, ideally leveraging insights from existing battery coating lines. At the same time, safety protocols, especially regarding handling of nanosheets and prevention of inhalation or environmental release, must align with industrial hygiene standards and regulations. Ensuring a smooth regulatory and environmental transition is integral. Regulatory frameworks such as REACH in the EU provide structured oversight for novel materials and must be considered early in process development. Safety data sheets for MXenes, waste treatment protocols, and end-of-life recovery plans should be designed in parallel to enable smooth commercialization. Finally, the field needs cross-disciplinary testbeds and pilot lines where MXene-enabled SSBs are validated at the cell level under realistic cycling conditions, manufacturing pace, and cost targets. Through iterative testing, measuring interfacial resistance evolution, critical current density stability, and retention of performance under thermal and mechanical stress, MXene technologies can mature from academic curiosity to robust industrial building blocks.

9. Conclusions

9.1. Summary of Key Findings

Over the past decade, MXenes have established themselves as one of the most versatile classes of two-dimensional materials for solid-state batteries (SSBs). Their unique combination of metallic electrical conductivity, high specific surface area, tunable surface chemistry, and mechanical resilience enables functions that extend far beyond those of conventional carbon additives. As this review has discussed, MXenes have demonstrated remarkable potential in multiple components of SSB architectures: as anodes, they offer high specific capacities and favorable Li^+ intercalation pathways; as cathode additives, they enhance electronic conductivity, alleviate sluggish charge transport, and enable high sulfur or high-nickel loading; as interfacial layers, they mitigate mechanical and chemical incompatibilities between Li-metal anodes and solid electrolytes, while also suppressing dendrite nucleation and growth; and as functional fillers in solid polymer and composite electrolytes, they contribute to enhanced Li^+ transference numbers, improved thermal and mechanical stability, and reduced grain-boundary resistance. The broad compositional versatility of MXenes further underpins their importance. Titanium-based MXenes remain the most widely explored due to precursor availability and favorable conductivity, but the emergence of DTM MXenes has expanded the chemical design space, enabling new opportunities for tuning redox activity, interlayer spacing, and interfacial affinity. In parallel, theoretical and computational studies, particularly DFT and high-throughput screening approaches, have clarified how surface terminations, defect chemistry, and heterostructure design directly influence Li^+ adsorption energetics and migration barriers. These insights provide a predictive framework that complements experimental optimization and reduces reliance on purely empirical trial-and-error strategies. Equally significant are the advances in synthetic methodologies and stabilization approaches. Fluoride-free etching strategies, molten-salt routes, and electrochemical methods are actively mitigating the environmental and safety risks associated with hydrofluoric acid. Meanwhile, the discovery of termination control, antioxidant-assisted colloidal stabilization, and protective coatings has substantially extended MXene shelf life, with some hybrid films remaining stable for months without significant conductivity loss. Together, these developments highlight that MXenes are not only functional nanomaterials but also increasingly engineered components with tunable, durable properties suitable for the stringent demands of SSBs.

9.2. Outlook on MXenes as Enablers of Next-Generation SSB Technologies

Despite their promise, the path toward large-scale industrial implementation of MXene-enabled SSBs remains challenging. The cost of producing high-quality MXenes, currently estimated at hundreds of dollars per kilogram at laboratory scale, is still far above the price of conventional conductive carbons. Achieving cost parity will require breakthroughs in precursor synthesis, waste minimization, and solvent recycling strategies, as highlighted in recent techno-economic and life-cycle assessments [145,166]. Parallel to this, establishing reproducible and standardized processing protocols is critical. While methods such as blade coating and roll-to-roll filtration of MXene inks have been demonstrated, scaling these techniques under the oxygen- and moisture-free conditions required for SSB production will demand significant investment in infrastructure and process optimization [148,168]. At the materials level, synergistic hybrid architectures are expected to dominate the next stage of development. Incorporating MXenes with polymers, sulfides, halides, and metal–organic frameworks provides a multi-functional strategy: MXenes can deliver lateral electronic conductivity, while the co-components provide vertical Li^+ conduction pathways and chemical stabilization. For instance, MOF-decorated MXenes have already been shown to combine high ionic conductivity (~4.4 mS cm^{-1}) and Li^+ transfer-

ence numbers of ~0.76, alongside mechanical reinforcement and flame retardancy, directly addressing safety and performance requirements for SSB electrolytes [160]. Similarly, DTM MXenes such as Mo_2TiC_2 or $Ti_xTa_{4-x}C_3$ exhibit expanded interlayer spacing and enhanced ion transport properties, offering pathways to overcome dendrite growth and sluggish diffusion [156,162]. The integration of MXenes with sulfide and halide-based electrolytes represents another frontier. These electrolytes provide exceptional ionic conductivities (often $>10^{-3}$ S cm^{-1}) but are highly sensitive to moisture and prone to interfacial degradation. Studies combining MXene interlayers with sulfide SSEs or hybrid polymer–sulfide matrices have demonstrated improved interfacial compatibility and reduced interphase resistance [163]. At the same time, spectroscopic and computational investigations have elucidated how MXene surfaces interact with sulfide species at the atomic level, pointing toward rational functionalization strategies that could further extend stability [164]. Ultimately, the roadmap toward commercialization requires a convergence of multiple factors: (i) the scale-up of fluoride-free and cost-effective MXene synthesis methods; (ii) integration into existing gigafactory-compatible coating and lamination processes; (iii) the design of heterostructures and DTM MXenes optimized for electrochemical performance and interfacial stability; and (iv) the alignment with environmental and regulatory frameworks such as the EU REACH regulation, ensuring safe production, handling, and end-of-life management [169]. If these challenges are successfully addressed, MXenes could transition from laboratory research materials into industrial-grade enablers of high-energy, safe, and durable SSB technologies, paving the way toward widespread deployment of next-generation batteries.

Funding: Financial support from NSF Center for the Advancement of Wearable Technologies-CAWT (Grant 1849243) and from the Consortium of Hybrid Resilient Energy Systems CHRES (DE-NA0003982) is gratefully acknowledged.

Institutional Review Board Statement: Not applicable.

Informed Consent Statement: Not applicable.

Data Availability Statement: The data is contained in the article and is available from the corresponding authors on reasonable request.

Acknowledgments: The author gratefully acknowledges Raúl S. García, Dina Márquez, and Dock García for their valuable assistance in organizing and updating the research databases, as well as for their support in coordinating the bibliography.

Conflicts of Interest: The author declares no conflicts of interest.

Abbreviations

The following abbreviations are used in this manuscript:

ALD	Atomic Layer Deposition
BC	Carbon Black
BN	Boron Nitride
CCD	Critical Current Density
CNT	Carbon Nanotube
COF	Covalent Organic Framework
CTAB	Cetyltrimethylammonium Bromide
CVD	Chemical Vapor Deposition
DE	Delamination Efficiency
DFT	Density Functional Theory
DMF	Dimethylformamide

DMSO	Dimethyl Sulfoxide
DTM	Double Transition Metal (MXene subclass)
EC	Ethylene Carbonate (also used for the European Commission in a regulatory context)
EELS	Electron Energy Loss Spectroscopy
EIS	Electrochemical Impedance Spectroscopy
EMI	1-Ethyl-3-methylimidazolium (ionic liquid cation)
EPA	United States Environmental Protection Agency
ESW	Electrochemical Stability Window
FEC	Fluoroethylene Carbonate (common electrolyte additive)
GCSE	Garnet-type Ceramic Solid Electrolyte
GO	Graphene Oxide
GWP	Global Warming Potential
LAMS	Lewis Acid Molten Salt (etching route for MXenes)
LATP	Lithium Aluminum Titanium Phosphate ($Li_{1.3}Al_{0.3}Ti_{1.7}(PO_4)_3$ solid electrolyte)
LCA	Life Cycle Assessment
LFP	Lithium Iron Phosphate
LGPS	Lithium Germanium Phosphorus Sulfide ($Li_{10}GeP_2S_{12}$ solid electrolyte)
LLZO	Lithium Lanthanum Zirconium Oxide ($Li_7La_3Zr_2O_{12}$ garnet-type SSE)
LLZTO	Lithium Lanthanum Zirconium Tantalum Oxide (doped garnet-type SSE)
MAX	Layered ternary carbides/nitrides ($M_{n+1}AX_n$ phases, where M = early transition metal, A = A-group element, X = C or N)
MOF	Metal–Organic Framework

References

1. Kerman, K.; Luntz, A.; Viswanathan, V.; Chiang, Y.-M.; Chen, Z. Review—Practical Challenges Hindering the Development of Solid State Li Ion Batteries. *J. Electrochem. Soc.* **2017**, *164*, A1731–A1744. [CrossRef]
2. Janek, J.; Zeier, W.G. A Solid Future for Battery Development. *Nat. Energy* **2016**, *1*, 16141. [CrossRef]
3. Kalnaus, S.; Dudney, N.J.; Westover, A.S.; Herbert, E.; Hackney, S. Solid-State Batteries: The Critical Role of Mechanics. *Science* **2023**, *381*, eabg5998. [CrossRef]
4. Zhang, Z.; Shao, Y.; Lotsch, B.; Hu, Y.-S.; Li, H.; Janek, J.; Nazar, L.F.; Nan, C.-W.; Maier, J.; Armand, M.; et al. New Horizons for Inorganic Solid State Ion Conductors. *Energy Environ. Sci.* **2018**, *11*, 1945–1976. [CrossRef]
5. Krauskopf, T.; Hartmann, H.; Zeier, W.G.; Janek, J. Toward a Fundamental Understanding of the Lithium Metal Anode in Solid-State Batteries—An Electrochemo-Mechanical Study on the Garnet-Type Solid Electrolyte $Li_{6.25}Al_{0.25}La_3Zr_2O_{12}$. *ACS Appl. Mater. Interfaces* **2019**, *11*, 14463–14477. [CrossRef]
6. Takada, K. Progress and Prospective of Solid-State Lithium Batteries. *Acta Mater.* **2013**, *61*, 759–770. [CrossRef]
7. Kato, Y.; Hori, S.; Saito, T.; Suzuki, K.; Hirayama, M.; Mitsui, A.; Yonemura, M.; Iba, H.; Kanno, R. High-Power All-Solid-State Batteries Using Sulfide Superionic Conductors. *Nat. Energy* **2016**, *1*, 16030. [CrossRef]
8. Thangadurai, V.; Narayanan, S.; Pinzaru, D. Garnet-Type Solid-State Fast Li Ion Conductors for Li Batteries: Critical Review. *Chem. Soc. Rev.* **2014**, *43*, 4714. [CrossRef]
9. Famprikis, T.; Canepa, P.; Dawson, J.A.; Islam, M.S.; Masquelier, C. Fundamentals of Inorganic Solid-State Electrolytes for Batteries. *Nat. Mater.* **2019**, *18*, 1278–1291. [CrossRef]
10. Naguib, M.; Kurtoglu, M.; Presser, V.; Lu, J.; Niu, J.; Heon, M.; Hultman, L.; Gogotsi, Y.; Barsoum, M.W. Two-Dimensional Nanocrystals Produced by Exfoliation of Ti_3AlC_2. *Adv. Mater.* **2011**, *23*, 4248–4253. [CrossRef] [PubMed]
11. Anasori, B.; Lukatskaya, M.R.; Gogotsi, Y. 2D Metal Carbides and Nitrides (MXenes) for Energy Storage. *Nat. Rev. Mater.* **2017**, *2*, 16098. [CrossRef]
12. Zhang, X.; Zhang, Z.; Zhou, Z. MXene-Based Materials for Electrochemical Energy Storage. *J. Energy Chem.* **2018**, *27*, 73–85. [CrossRef]
13. Gogotsi, Y.; Anasori, B. The Rise of MXenes. *ACS Nano* **2019**, *13*, 8491–8494. [CrossRef]
14. Ding, L.; Wei, Y.; Wang, Y.; Chen, H.; Caro, J.; Wang, H. A Two-Dimensional Lamellar Membrane: MXene Nanosheet Stacks. *Angew. Chem. Int. Ed.* **2017**, *56*, 1825–1829. [CrossRef] [PubMed]
15. Khazaei, M.; Ranjbar, A.; Arai, M.; Sasaki, T.; Yunoki, S. Electronic Properties and Applications of MXenes: A Theoretical Review. *J. Mater. Chem. C* **2017**, *5*, 2488–2503. [CrossRef]

16. Zhang, C.; Anasori, B.; Seral-Ascaso, A.; Park, S.; McEvoy, N.; Shmeliov, A.; Duesberg, G.S.; Coleman, J.N.; Gogotsi, Y.; Nicolosi, V. Transparent, Flexible, and Conductive 2D Titanium Carbide (MXene) Films with High Volumetric Capacitance. *Adv. Mater.* **2017**, *29*, 1702678. [CrossRef]
17. Lukatskaya, M.R.; Mashtalir, O.; Ren, C.E.; Dall'Agnese, Y.; Rozier, P.; Taberna, P.L.; Naguib, M.; Simon, P.; Barsoum, M.W.; Gogotsi, Y. Cation Intercalation and High Volumetric Capacitance of Two-Dimensional Titanium Carbide. *Science* **2013**, *341*, 1502–1505. [CrossRef] [PubMed]
18. Er, D.; Li, J.; Naguib, M.; Gogotsi, Y.; Shenoy, V.B. Ti_3C_2 MXene as a High Capacity Electrode Material for Metal (Li, Na, K, Ca) Ion Batteries. *ACS Appl. Mater. Interfaces* **2014**, *6*, 11173–11179. [CrossRef] [PubMed]
19. Lukatskaya, M.R.; Kota, S.; Lin, Z.; Zhao, M.-Q.; Shpigel, N.; Levi, M.D.; Halim, J.; Taberna, P.-L.; Barsoum, M.W.; Simon, P.; et al. Ultra-High-Rate Pseudocapacitive Energy Storage in Two-Dimensional Transition Metal Carbides. *Nat. Energy* **2017**, *2*, 17105. [CrossRef]
20. Belay Ibrahim, K.; Ahmed Shifa, T.; Zorzi, S.; Getaye Sendeku, M.; Moretti, E.; Vomiero, A. Emerging 2D Materials beyond Mxenes and TMDs: Transition Metal Carbo-Chalcogenides. *Prog. Mater. Sci.* **2024**, *144*, 101287. [CrossRef]
21. Xiao, Z.; Li, Z.; Meng, X.; Wang, R. MXene-Engineered Lithium–Sulfur Batteries. *J. Mater. Chem. A* **2019**, *7*, 22730–22743. [CrossRef]
22. Badawi, N.; Bhuyan, M.; Luqman, M.; Alshareef, R.S.; Rafe Hatshan, M.; Al-Warthan, A.; Farooq Adil, S. MXenes the Future of Solid-State Supercapacitors: Status, Challenges, Prospects, and Applications. *Arab. J. Chem.* **2024**, *17*, 105866. [CrossRef]
23. Li, X.; Huang, Z.; Shuck, C.E.; Liang, G.; Gogotsi, Y.; Zhi, C. MXene Chemistry, Electrochemistry and Energy Storage Applications. *Nat. Rev. Chem.* **2022**, *6*, 389–404. [CrossRef]
24. Long, M.Q.; Tang, K.K.; Xiao, J.; Li, J.Y.; Chen, J.; Gao, H.; Chen, W.H.; Liu, C.T.; Liu, H. Recent Advances on MXene Based Materials for Energy Storage Applications. *Mater. Today Sustain.* **2022**, *19*, 100163. [CrossRef]
25. Barsoum, M.W. *MAX Phases: Properties of Machinable Ternary Carbides and Nitrides*; Wiley-VCH: Hoboken, NJ, USA, 2013.
26. Borah, A.J.; Natu, V.; Biswas, A.; Srivastava, A. A Review on Recent Progress in Synthesis, Properties, and Applications of MXenes. *Oxf. Open Mater. Sci.* **2025**, *5*, itae017. [CrossRef]
27. Lipatov, A.; Alhabeb, M.; Lu, H.; Zhao, S.; Loes, M.J.; Vorobeva, N.S.; Dall'Agnese, Y.; Gao, Y.; Gruverman, A.; Gogotsi, Y.; et al. Electrical and Elastic Properties of Individual Single-Layer $Nb_4C_3T_x$ MXene Flakes. *Adv. Electron. Mater.* **2020**, *6*, 1901382. [CrossRef]
28. Hope, M.A.; Forse, A.C.; Griffith, K.J.; Lukatskaya, M.R.; Ghidiu, M.; Gogotsi, Y.; Grey, C.P. NMR Reveals the Surface Functionalisation of Ti_3C_2 MXene. *Phys. Chem. Chem. Phys.* **2016**, *18*, 5099–5102. [CrossRef]
29. Gouveia, J.D.; Gomes, J.R.B. Effect of Surface Composition on the Stability of Ti- and V-Based Oxycarbide and Oxynitride MXenes. *Mater. Today Phys.* **2024**, *46*, 101481. [CrossRef]
30. Du, W.; Yang, L.; Feng, J.; Zhu, W.; Li, J.; Zhang, P.; Ma, Q. Advancements in Methodologies and Techniques for the Synthesis of Energetic Materials: A Review. *Energetic Mater. Front.* **2024**, *5*, 175–190. [CrossRef]
31. Plaickner, J.; Petit, T.; Bärmann, P.; Schultz, T.; Koch, N.; Esser, N. Surface Termination Effects on Raman Spectra of $Ti_3C_2T_x$ MXenes: An in Situ UHV Analysis. *Phys. Chem. Chem. Phys.* **2024**, *26*, 20883–20890. [CrossRef]
32. Zhang, C.; Ma, Y.; Zhang, X.; Abdolhosseinzadeh, S.; Sheng, H.; Lan, W.; Pakdel, A.; Heier, J.; Nüesch, F. Two-Dimensional Transition Metal Carbides and Nitrides (MXenes): Synthesis, Properties, and Electrochemical Energy Storage Applications. *Energy Environ. Mater.* **2020**, *3*, 29–55. [CrossRef]
33. Alhabeb, M.; Maleski, K.; Anasori, B.; Lelyukh, P.; Clark, L.; Sin, S.; Gogotsi, Y. Guidelines for Synthesis and Processing of Two-Dimensional Titanium Carbide ($Ti_3C_2T_x$ MXene). *Chem. Mater.* **2017**, *29*, 7633–7644. [CrossRef]
34. Shekhirev, M.; Busa, J.; Shuck, C.E.; Torres, A.; Bagheri, S.; Sinitskii, A.; Gogotsi, Y. Ultralarge Flakes of $Ti_3C_2T_x$ MXene via Soft Delamination. *ACS Nano* **2022**, *16*, 13695–13703. [CrossRef]
35. Shuck, C.E.; Sarycheva, A.; Anayee, M.; Levitt, A.; Zhu, Y.; Uzun, S.; Balitskiy, V.; Zahorodna, V.; Gogotsi, O.; Gogotsi, Y. Scalable Synthesis of $Ti_3C_2T_x$ MXene. *Adv. Eng. Mater.* **2020**, *22*, 1901241. [CrossRef]
36. Ghidiu, M.; Lukatskaya, M.R.; Zhao, M.-Q.; Gogotsi, Y.; Barsoum, M.W. Conductive Two-Dimensional Titanium Carbide 'Clay' with High Volumetric Capacitance. *Nature* **2014**, *516*, 78–81. [CrossRef]
37. Mashtalir, O.; Naguib, M.; Mochalin, V.N.; Dall'Agnese, Y.; Heon, M.; Barsoum, M.W.; Gogotsi, Y. Intercalation and Delamination of Layered Carbides and Carbonitrides. *Nat. Commun.* **2013**, *4*, 1716. [CrossRef]
38. Li, T.; Yao, L.; Liu, Q.; Gu, J.; Luo, R.; Li, J.; Yan, X.; Wang, W.; Liu, P.; Chen, B.; et al. Fluorine-Free Synthesis of High-Purity $Ti_3C_2T_x$ (T=OH, O) via Alkali Treatment. *Angew. Chem. Int. Ed.* **2018**, *57*, 6115–6119. [CrossRef]
39. Kruger, D.D.; García, H.; Primo, A. Molten Salt Derived MXenes: Synthesis and Applications. *Adv. Sci.* **2024**, *11*, 2307106. [CrossRef]
40. Kareem, S.A.; Ibrahim, M.A.; Anaele, J.U.; Olanrewaju, O.F.; Aikulola, E.O.; Bodunrin, M.O. Recent Advances in Machine Learning Applications for MXene Materials: Design, Synthesis, Characterization, and Commercialization for Energy and Environmental Applications. *Next Mater.* **2025**, *8*, 100864. [CrossRef]

41. Rasheed, T.; Shafi, S.; Anwar, M.T.; Ahmad, R.; Ahmad, M.S.; Usman, M.; Fawy, K.F. MXenes: Transforming Advanced Materials through Electrochemical Reduction Reactions—Opportunities and Challenges. *Chem. Eng. J.* **2025**, *506*, 159926. [CrossRef]
42. Naguib, M.; Come, J.; Dyatkin, B.; Presser, V.; Taberna, P.-L.; Simon, P.; Barsoum, M.W.; Gogotsi, Y. MXene: A Promising Transition Metal Carbide Anode for Lithium-Ion Batteries. *Electrochem. Commun.* **2012**, *16*, 61–64. [CrossRef]
43. Peng, C.; Wei, P.; Chen, X.; Zhang, Y.; Zhu, F.; Cao, Y.; Wang, H.; Yu, H.; Peng, F. A Hydrothermal Etching Route to Synthesis of 2D MXene (Ti_3C_2, Nb_2C): Enhanced Exfoliation and Improved Adsorption Performance. *Ceram. Int.* **2018**, *44*, 18886–18893. [CrossRef]
44. Li, M.; Lu, J.; Luo, K.; Li, Y.; Chang, K.; Chen, K.; Zhou, J.; Rosen, J.; Hultman, L.; Eklund, P.; et al. Element Replacement Approach by Reaction with Lewis Acidic Molten Salts to Synthesize Nanolaminated MAX Phases and MXenes. *J. Am. Chem. Soc.* **2019**, *141*, 4730–4737. [CrossRef]
45. Khazaei, M.; Arai, M.; Sasaki, T.; Chung, C.; Venkataramanan, N.S.; Estili, M.; Sakka, Y.; Kawazoe, Y. Novel Electronic and Magnetic Properties of Two-Dimensional Transition Metal Carbides and Nitrides. *Adv. Funct. Mater.* **2013**, *23*, 2185–2192. [CrossRef]
46. Chy, M.N.U.; Rahman, M.A.; Kim, J.-H.; Barua, N.; Dujana, W.A. MXene as Promising Anode Material for High-Performance Lithium-Ion Batteries: A Comprehensive Review. *Nanomaterials* **2024**, *14*, 616. [CrossRef] [PubMed]
47. Shi, X.; Guo, F.; Hou, K.; Guan, G.; Lu, L.; Zhang, Y.; Xu, J.; Shang, Y. Highly Flexible All-Solid-State Supercapacitors Based on MXene/CNT Composites. *Energy Fuels* **2023**, *37*, 9704–9712. [CrossRef]
48. Zachariah, S.; Indirajith, R.; Rajalakshmi, M. Recent Advances in Optoelectronic Properties and Applications of $Ti_3C_2T_x$ MXene. *J. Alloys Compd.* **2025**, *1011*, 178296. [CrossRef]
49. Voiry, D.; Mohite, A.; Chhowalla, M. Phase Engineering of Transition Metal Dichalcogenides. *Chem. Soc. Rev.* **2015**, *44*, 2702–2712. [CrossRef]
50. Wang, G. MXene-Enabled Interfaces and Architectures for High-Performance Zinc Anodes in Aqueous Zinc-Ion Batteries. *Int. J. Electrochem. Sci.* **2025**, *20*, 101023. [CrossRef]
51. Man, Q.; An, Y.; Shen, H.; Wei, C.; Zhang, X.; Wang, Z.; Xiong, S.; Feng, J. MXenes and Their Derivatives for Advanced Solid-State Energy Storage Devices. *Adv. Funct. Mater.* **2023**, *33*, 2303668. [CrossRef]
52. Protyai, M.I.H.; Bin Rashid, A. A comprehensive overview of recent progress in MXene-based polymer composites: Their fabrication processes, advanced applications, and prospects. *Heliyon* **2024**, *10*, e37030. [CrossRef]
53. Pan, Q.; Zheng, Y.; Kota, S.; Huang, W.; Wang, S.; Qi, H.; Kim, S.; Tu, Y.; Barsoum, M.W.; Li, C.Y. 2D MXene-Containing Polymer Electrolytes for All-Solid-State Lithium Metal Batteries. *Nanoscale Adv.* **2019**, *1*, 395–402. [CrossRef] [PubMed]
54. Sarfraz, N.; Kanwal, N.; Ali, M.; Ali, K.; Hasnain, A.; Ashraf, M.; Ayaz, M.; Ifthikar, J.; Ali, S.; Hendi, A.; et al. Materials Advancements in Solid-State Inorganic Electrolytes for Highly Anticipated All Solid Li-Ion Batteries. *Energy Storage Mater.* **2024**, *71*, 103619. [CrossRef]
55. Yu, R. Recent Advances of Sulfide Electrolytes in All-Solid-State Lithium Batteries. *MATEC Web Conf.* **2025**, *410*, 01030. [CrossRef]
56. Jacob, M.; Moreno Fernández, H.; Haben, A.; Waidha, A.I.; Özel, S.; Hofmann, J.P.; Kautenburger, R.; Clemens, O.; Wissel, K. Direct Recycling of All-Solid-State Batteries with a Halide Solid Electrolyte via Water-Based Separation: Interactions of Electrode Materials in Aqueous Li_3 $InCl_6$ Solutions. *Batter. Supercaps* **2025**, 2500189. [CrossRef]
57. Munir, M.A.; Khalid, S. Focused Review on the Synthesis of Titanium Carbide MXene via Fluorine-Free Methods for Lithium-Ion Batteries. *Energy Fuels* **2025**, *39*, 2889–2915. [CrossRef]
58. Wu, B.; Chen, C.; Danilov, D.L.; Eichel, R.-A.; Notten, P.H.L. All-Solid-State Thin Film Li-Ion Batteries: New Challenges, New Materials, and New Designs. *Batteries* **2023**, *9*, 186. [CrossRef]
59. Yang, K.; Liu, Y.; Zhao, F.; Li, J.; Yang, H.; Wang, Y.; He, Y. Multifunction of MXene in Lithium–Sulfur Batteries: A Review. *Energy Fuels* **2024**, *38*, 13837–13857. [CrossRef]
60. Xu, H.; Liu, S.; Li, Z.; Ding, F.; Wang, T.; Liu, T.; Wang, W.; Song, K.; Liu, J.; Hu, L. $Ti_3C_2T_x$ MXene Enhanced PEO/SN-Based Solid Electrolyte for High-Performance Li Metal Battery. *J. Mater. Sci. Technol.* **2025**, *219*, 101–112. [CrossRef]
61. Zarepour, A.; Ahmadi, S.; Rabiee, N.; Zarrabi, A.; Iravani, S. Self-Healing MXene- and Graphene-Based Composites: Properties and Applications. *Nano-Micro Lett.* **2023**, *15*, 100. [CrossRef]
62. Hu, M.; Chen, L.; Jing, Y.; Zhu, Y.; Dai, J.; Meng, A.; Sun, C.; Jia, J.; Li, Z. Intensifying Electrochemical Activity of Ti3C2Tx MXene via Customized Interlayer Structure and Surface Chemistry. *Molecules* **2023**, *28*, 5776. [CrossRef] [PubMed]
63. Lin, Z.; Rozier, P.; Duployer, B.; Taberna, P.-L.; Anasori, B.; Gogotsi, Y.; Simon, P. Electrochemical and In-Situ X-Ray Diffraction Studies of $Ti_3C_2T_x$ MXene in Ionic Liquid Electrolyte. *Electrochem. Commun.* **2016**, *72*, 50–53. [CrossRef]
64. Zhang, Q.; Zhang, X.; Xiao, Y.; Li, C.; Tan, H.H.; Liu, J.; Wu, Y. Theoretical Insights into the Favorable Functionalized Ti_2C-Based MXenes for Lithium–Sulfur Batteries. *ACS Omega* **2020**, *5*, 29272–29283. [CrossRef]
65. Kiai, M.S.; Aslfattahi, N.; Karatas, D.; Baydogan, N.; Samylingam, L.; Kadirgama, K.; Kok, C.K. Experimental and DFT Investigations on Multifunctional $Ti_3C_2T_x$ MXenes/PDAAQ Free Standing Interlayer for Enhancing the Cycle Life and High-Rate Performance of Na–S Batteries. *J. Phys. Chem. Solids* **2025**, *208*, 113083. [CrossRef]

66. Gentile, A.; Pianta, N.; Fracchia, M.; Pollastri, S.; Ferrara, C.; Marchionna, S.; Aquilanti, G.; Tosoni, S.; Ghigna, P.; Ruffo, R. $Ti_3C_2T_x$ MXenes as Anodes for Sodium-Ion Batteries: The In Situ Comprehension of the Electrode Reaction. *ACS Appl. Energy Mater.* **2025**, *8*, 2229–2238. [CrossRef] [PubMed]
67. Shon, H.K.; Askari, M.; Merenda, A.; Shah, D.; Tijing, L. High-Capacity and Selective Lithium-Ion Recovery Via Ti3C2Tx @Sno2 Composite Electrodes Using Hybrid Capacitive Deionization. 2025. Available online: https://papers.ssrn.com/sol3/papers.cfm?abstract_id=5273042 (accessed on 23 August 2025).
68. Shreenag Meda, U.; Madan Raikar, O.; Adaguru Rudregowda, C.; Rangappa, D.; Rani, N.; Ranga, S.S.; Pandey, A. MXenes as Versatile Materials for Hydrogen Technology and Multifunctional Applications. *Chem. Asian J.* **2025**, *20*, e202401678. [CrossRef] [PubMed]
69. VahidMohammadi, A.; Rosen, J.; Gogotsi, Y. The World of Two-Dimensional Carbides and Nitrides (MXenes). *Science* **2021**, *372*, eabf1581. [CrossRef] [PubMed]
70. Machín, A.; Morant, C.; Márquez, F. Advancements and Challenges in Solid-State Battery Technology: An In-Depth Review of Solid Electrolytes and Anode Innovations. *Batteries* **2024**, *10*, 29. [CrossRef]
71. Kitchamsetti, N.; Han, H.; Mhin, S. MXenes and MXene-Based Composites: Preparation, Characteristics, Theoretical Investigations, and Application in Developing Sulfur Cathodes, Lithium Anodes, and Functional Separators for Lithium–Sulfur Batteries. *Batteries* **2025**, *11*, 206. [CrossRef]
72. Liang, X.; Garsuch, A.; Nazar, L.F. Sulfur Cathodes Based on Conductive MXene Nanosheets for High-Performance Lithium–Sulfur Batteries. *Angew. Chem. Int. Ed.* **2015**, *54*, 3907–3911. [CrossRef]
73. Zhang, Y.; Wang, Y.; Jiang, Q.; El-Demellawi, J.K.; Kim, H.; Alshareef, H.N. MXene Printing and Patterned Coating for Device Applications. *Adv. Mater.* **2020**, *32*, 1908486. [CrossRef] [PubMed]
74. Liu, R.; Li, C.; Li, Q.; Zhang, S.; Wang, C.; Zhang, Z.; Shi, Y.; Yang, L.; Yin, L.; Wang, R. High Performance All-Solid-State Li–Se Battery Based on Selenium Loaded on Ti_3C_2 MXene Cathode. *Green Energy Resour.* **2024**, *2*, 100058. [CrossRef]
75. Zhang, P.; Wang, X.; Zhang, Y.; Wei, Y.; Shen, N.; Chen, S.; Xu, B. Burgeoning Silicon/MXene Nanocomposites for Lithium Ion Batteries: A Review. *Adv. Funct. Mater.* **2024**, *34*, 2402307. [CrossRef]
76. Jiang, X.; Tang, C.; Zhou, X.; Hou, J.; Jiang, S.; Meng, L.; Zhang, Y. Recent Progress in Si/$Ti_3C_2T_x$ MXene Anode Materials for Lithium-Ion Batteries. *iScience* **2024**, *27*, 111217. [CrossRef] [PubMed]
77. Myint, W.; Lolupiman, K.; Yang, C.; Woottapanit, P.; Limphirat, W.; Kidkhunthod, P.; Muzakir, M.; Karnan, M.; Zhang, X.; Qin, J. Exploring the Electrochemical Superiority of V_2O_5/TiO_2@Ti_3C_2-MXene Hybrid Nanostructures for Enhanced Lithium-Ion Battery Performance. *ACS Appl. Mater. Interfaces* **2024**, *16*, 53764–53774. [CrossRef]
78. Tang, L.; Zhang, L.; Yin, G.; Tao, X.; Yu, L.; Wang, X.; Sun, C.; Sun, Y.; Hong, E.; Zhao, G.; et al. 2D Porous Ti3C2 MXene as Anode Material for Sodium-Ion Batteries with Excellent Reaction Kinetics. *Molecules* **2025**, *30*, 1100. [CrossRef]
79. Tang, X.; Zhou, D.; Li, P.; Guo, X.; Wang, C.; Kang, F.; Li, B.; Wang, G. High-Performance Quasi-Solid-State MXene-Based Li–I Batteries. *ACS Cent. Sci.* **2019**, *5*, 365–373. [CrossRef]
80. García, R.E.; Chiang, Y.-M.; Craig Carter, W.; Limthongkul, P.; Bishop, C.M. Microstructural Modeling and Design of Rechargeable Lithium-Ion Batteries. *J. Electrochem. Soc.* **2005**, *152*, A255. [CrossRef]
81. Sharafi, A.; Kazyak, E.; Davis, A.L.; Yu, S.; Thompson, T.; Siegel, D.J.; Dasgupta, N.P.; Sakamoto, J. Surface Chemistry Mechanism of Ultra-Low Interfacial Resistance in the Solid-State Electrolyte $Li_7La_3Zr_2O_{12}$. *Chem. Mater.* **2017**, *29*, 7961–7968. [CrossRef]
82. Porz, L.; Swamy, T.; Sheldon, B.W.; Rettenwander, D.; Frömling, T.; Thaman, H.L.; Berendts, S.; Uecker, R.; Carter, W.C.; Chiang, Y. Mechanism of Lithium Metal Penetration through Inorganic Solid Electrolytes. *Adv. Energy Mater.* **2017**, *7*, 1701003. [CrossRef]
83. Kazyak, E.; Garcia-Mendez, R.; LePage, W.S.; Sharafi, A.; Davis, A.L.; Sanchez, A.J.; Chen, K.-H.; Haslam, C.; Sakamoto, J.; Dasgupta, N.P. Li Penetration in Ceramic Solid Electrolytes: Operando Microscopy Analysis of Morphology, Propagation, and Reversibility. *Matter* **2020**, *2*, 1025–1048. [CrossRef]
84. Harry, K.J.; Hallinan, D.T.; Parkinson, D.Y.; MacDowell, A.A.; Balsara, N.P. Detection of Subsurface Structures underneath Dendrites Formed on Cycled Lithium Metal Electrodes. *Nat. Mater.* **2014**, *13*, 69–73. [CrossRef]
85. Liu, M.; Song, A.; Zhang, X.; Wang, J.; Fan, Y.; Wang, G.; Tian, H.; Ma, Z.; Shao, G. Interfacial Lithium-Ion Transportation in Solid-State Batteries: Challenges and Prospects. *Nano Energy* **2025**, *136*, 110749. [CrossRef]
86. Lou, S.; Yu, Z.; Liu, Q.; Wang, H.; Chen, M.; Wang, J. Multi-Scale Imaging of Solid-State Battery Interfaces: From Atomic Scale to Macroscopic Scale. *Chem* **2020**, *6*, 2199–2218. [CrossRef]
87. Strauss, F.; Kitsche, D.; Ma, Y.; Teo, J.H.; Goonetilleke, D.; Janek, J.; Bianchini, M.; Brezesinski, T. Operando Characterization Techniques for All-Solid-State Lithium-Ion Batteries. *Adv. Energy Sustain. Res.* **2021**, *2*, 2100004. [CrossRef]
88. Huang, J.; Wu, K.; Xu, G.; Wu, M.; Dou, S.; Wu, C. Recent Progress and Strategic Perspectives of Inorganic Solid Electrolytes: Fundamentals, Modifications, and Applications in Sodium Metal Batteries. *Chem. Soc. Rev.* **2023**, *52*, 4933–4995. [CrossRef]
89. Liu, C.; Yuan, Z.; Chen, K.; Jiang, Y.; Yue, M.; Dong, K.; Liu, Y.; Guo, Y.; Wang, Y. MXene-BN-Introduced Artificial SEI to Inhibit Dendrite Growth of Lithium Metal Batteries. *ACS Appl. Mater. Interfaces* **2023**, *15*, 56356–56364. [CrossRef]

90. Mao, Y.; Liu, J.; Chen, W.; Zhang, W.; Sun, C. Recent Advances in Garnet-Based Electrolytes for Solid-State Lithium Metal Batteries: Interfacial Challenges and Engineering Strategies. *Mater. Horiz.* **2025**, *12*, 6082–6123. [CrossRef] [PubMed]
91. Li, X.; Zhang, Z.; Chen, D.; Ma, F.; Huang, J.; Wang, Y.; Wang, L.; Wu, Y.; Chen, Y. A Dual-Protective MXene/COF Artificial Interface for Dendrite-Free and Stable Lithium Metal Anodes. *Adv. Funct. Mater.* **2025**, 2505390. [CrossRef]
92. Li, X.L.; Lieu, W.Y.; Wang, L.; Yan, D.; Li, Y.; Ghosh, T.; Li, Y.; Lu, J.; Seh, Z.W.; Yang, H.Y. Silver-Atom Modulation of Ti Vacancies in MXene Enables Uniform Spherical Lithium Deposition. *ACS Energy Lett.* **2024**, *9*, 4929–4938. [CrossRef]
93. Ha, S.; Kim, D.; Lim, H.; Koo, C.M.; Kim, S.J.; Yun, Y.S. Lithiophilic MXene-Guided Lithium Metal Nucleation and Growth Behavior. *Adv. Funct. Mater.* **2021**, *31*, 2101261. [CrossRef]
94. Tao, F.; Xie, D.; Diao, W.-Y.; Liu, C.; Sun, H.-Z.; Li, W.-L.; Zhang, J.-P.; Wu, X.-L. Highly Lithiophilic $Ti_3C_2T_x$-Mxene Anchored on a Flexible Carbon Foam Scaffolds as the Basis for a Dendrite-Free Lithium Metal Anode. *New Carbon. Mater.* **2023**, *38*, 765–773. [CrossRef]
95. Yoon, J.; Chae, O.B.; Wu, M.; Jung, H.-T. Dual-Functional Surface of MXene Anodes Boosts Long-Term Cyclability of Lithium-Metal Batteries. *J. Mater. Chem. A* **2025**, *13*, 17511–17518. [CrossRef]
96. Zeng, X.; Mahato, M.; Oh, W.; Yoo, H.; Nguyen, V.H.; Oh, S.; Valurouthu, G.; Jeong, S.; Ahn, C.W.; Gogotsi, Y.; et al. Stoichiometric Ti3C2T_xCoating for Inhibiting Dendrite Growth in Anode-Free Lithium Metal Batteries. *Energy Environ. Mater.* **2024**, *7*, e12686. [CrossRef]
97. Wei, C.; Wang, Y.; Zhang, Y.; Tan, L.; Qian, Y.; Tao, Y.; Xiong, S.; Feng, J. Flexible and Stable 3D Lithium Metal Anodes Based on Self-Standing MXene/COF Frameworks for High-Performance Lithium-Sulfur Batteries. *Nano Res.* **2021**, *14*, 3576–3584. [CrossRef]
98. Zhang, X.; Lv, R.; Wang, A.; Guo, W.; Liu, X.; Luo, J. MXene Aerogel Scaffolds for High-Rate Lithium Metal Anodes. *Angew. Chem. Int. Ed.* **2018**, *57*, 15028–15033. [CrossRef]
99. Zhang, B.; Ju, Z.; Xie, Q.; Luo, J.; Du, L.; Zhang, C.; Tao, X. Ti_3CNT_x MXene/rGO Scaffolds Directing the Formation of a Robust, Layered SEI toward High-Rate and Long-Cycle Lithium Metal Batteries. *Energy Storage Mater.* **2023**, *58*, 322–331. [CrossRef]
100. Wei, C.; Tao, Y.; An, Y.; Tian, Y.; Zhang, Y.; Feng, J.; Qian, Y. Recent Advances of Emerging 2D MXene for Stable and Dendrite-Free Metal Anodes. *Adv. Funct. Mater.* **2020**, *30*, 2004613. [CrossRef]
101. Mao, Y.-Q.; Dong, G.-H.; Zhu, W.-B.; Li, Y.-Q.; Huang, P.; Fu, S.-Y. Novel Sandwich Structured Glass Fiber Cloth/Poly(Ethylene Oxide)-Mxene Composite Electrolyte. *Nano Materials Sci.* **2024**, *6*, 60–67. [CrossRef]
102. Vijayananth, K.; Palaniappan, S.K.; Singh, M.K.; Pudhupalayam Muthukutti, G.; Mavinkere Rangappa, S.; Siengchin, S. Exploring MXene-Polymer Composites for Mechanical, Tribological, and EMI Shielding Applications. *Polym. Compos.* **2025**, 1–24. [CrossRef]
103. Yang, X.; Liu, J.; Pei, N.; Chen, Z.; Li, R.; Fu, L.; Zhang, P.; Zhao, J. The Critical Role of Fillers in Composite Polymer Electrolytes for Lithium Battery. *Nano-Micro Lett.* **2023**, *15*, 74. [CrossRef] [PubMed]
104. Du, X.; Tian, S.; Liu, T.; Yang, M.; Song, B.; Zhang, W. MXene-Coordinated Polymer Electrolytes for High-Performance Solid-State Lithium Metal Batteries. *Chem. Eng. J.* **2025**, *522*, 168030. [CrossRef]
105. Narayanasamy, M.; Zaman, S.; Koo, C.M. 2D MXenes for All-Solid-State Batteries: A Comprehensive Review. *Mater. Today Energy* **2023**, *37*, 101405. [CrossRef]
106. Hadad, S.; Hamrahjoo, M.; Khezraqa, H.; Golshan, M.; Wang, Z.; Salami-Kalajahi, M. Starch Acetate Grafted to MXene Composite Surpasses Room Temperature Liquid Electrolyte Performance for All-Solid-State Lithium-Ion Batteries. *Adv. Sci.* **2025**, *12*, e03285. [CrossRef]
107. Likitaporn, C.; Okhawilai, M.; Kasemsiri, P.; Qin, J.; Potiyaraj, P.; Uyama, H. High Electrolyte Uptake of MXene Integrated Membrane Separators for Zn-Ion Batteries. *Sci. Rep.* **2022**, *12*, 19915. [CrossRef]
108. Lee, A.; Shekhirev, M.; Anayee, M.; Gogotsi, Y. Multi-Year Study of Environmental Stability of $Ti_3C_2T_x$ MXene Films. *Graphene 2D Mater.* **2024**, *9*, 77–85. [CrossRef]
109. Serajian, S.; Shamsabadi, A.A.; Gnani Peer Mohamed, S.I.; Nejati, S.; Bavarian, M. MXenes in Solid-State Batteries: Current Status and Outlook. *J. Power Sources* **2024**, *610*, 234721. [CrossRef]
110. Sharma, V.; Datta, D. Variation in Interface Strength of Silicon with Surface Engineered Ti_3C_2 MXenes. *arXiv* **2020**. [CrossRef]
111. Xu, L.; Wu, T.; Kent, P.R.C.; Jiang, D. Interfacial Charge Transfer and Interaction in the MXene/TiO_2 Heterostructures. *arXiv* **2021**. [CrossRef]
112. Xiao, Y.; Wang, Y.; Bo, S.-H.; Kim, J.C.; Miara, L.J.; Ceder, G. Understanding Interface Stability in Solid-State Batteries. *Nat. Rev. Mater.* **2019**, *5*, 105–126. [CrossRef]
113. Byeon, Y.-W.; Kim, H. Review on Interface and Interphase Issues in Sulfide Solid-State Electrolytes for All-Solid-State Li-Metal Batteries. *Electrochem* **2021**, *2*, 452–471. [CrossRef]
114. Wang, S.; Fang, R.; Li, Y.; Liu, Y.; Xin, C.; Richter, F.H.; Nan, C.-W. Interfacial Challenges for All-Solid-State Batteries Based on Sulfide Solid Electrolytes. *J. Mater.* **2021**, *7*, 209–218. [CrossRef]

115. Qi, Y.; Swift, M.W.; Fuller, E.J.; Talin, A.A. Interface Potentials inside Solid-State Batteries: Origins and Implications. *MRS Bull.* **2023**, *48*, 1239–1246. [CrossRef]
116. Wen, J.; Huang, L.; Huang, Y.; Luo, W.; Huo, H.; Wang, Z.; Zheng, X.; Wen, Z.; Huang, Y. A Lithium-MXene Composite Anode with High Specific Capacity and Low Interfacial Resistance for Solid-State Batteries. *Energy Storage Mater.* **2022**, *45*, 934–940. [CrossRef]
117. Kawai, K.; Lee, H.; Nomura, Y.; Fujita, M.; Kitaura, H.; Hosono, E.; Nakajima, H.; Tsukasaki, H.; Mori, S.; Sakuda, A.; et al. MXene Electrodes for All Strain-Free Solid-State Batteries. *ACS Appl. Mater. Interfaces* **2024**, *16*, 57377–57385. [CrossRef] [PubMed]
118. Ding, N.; Shi, X.; Liao, S.; Liu, M.; Xu, Y.; Li, Z.; Liu, J.; Li, X. Structural Design and Investigation of Ti_3C_2 MXene as a Conductive Interlayer for Improving the Lithium-Storage Performance of PSi@C Anode Material. *Electrochim. Acta* **2024**, *508*, 145216. [CrossRef]
119. Han, X.; Zhou, W.; Chen, M.; Chen, J.; Wang, G.; Liu, B.; Luo, L.; Chen, S.; Zhang, Q.; Shi, S.; et al. Interfacial Nitrogen Engineering of Robust Silicon/MXene Anode toward High Energy Solid-State Lithium-Ion Batteries. *J. Energy Chem.* **2022**, *67*, 727–735. [CrossRef]
120. Wang, Y.; Yuan, P.; Xu, Z.; Liu, X.-X.; Feng, S.; Cao, M.; Cao, C.; Wang, X.; Pan, L.; Sun, Z.-M. $Ti_3C_2T_x$ MXene In-Situ Transformed Li_2TiO_3 Interface Layer Enabling 4.5 V-$LiCoO_2$/Sulfide All-Solid-State Lithium Batteries with Superior Rate Capability and Cyclability. *Chin. Chem. Lett.* **2024**, *35*, 108776. [CrossRef]
121. Coley, W.; Akhavi, A.-A.; Pena, P.; Shang, R.; Ma, Y.; Moseni, K.; Ozkan, M.; Ozkan, C.S. Charging the Future with Pioneering MXenes: Scalable 2D Materials for Next-Generation Batteries. *Nanomaterials* **2025**, *15*, 1089. [CrossRef]
122. Ren, F.; Liang, Z.; Zhao, W.; Zuo, W.; Lin, M.; Wu, Y.; Yang, X.; Gong, Z.; Yang, Y. The Nature and Suppression Strategies of Interfacial Reactions in All-Solid-State Batteries. *Energy Environ. Sci.* **2023**, *16*, 2579–2590. [CrossRef]
123. Jayan, R.; Islam, M.M. Functionalized MXenes as Effective Polyselenides Immobilizer for Lithium-Selenium Batteries: A Density Functional Theory (DFT) Study. *arXiv* **2020**. [CrossRef]
124. Ali, I.; Faraz Ud Din, M.; Gu, Z.-G. MXenes Thin Films: From Fabrication to Their Applications. *Molecules* **2022**, *27*, 4925. [CrossRef] [PubMed]
125. Guo, T.; Zhou, D.; Deng, S.; Jafarpour, M.; Avaro, J.; Neels, A.; Heier, J.; Zhang, C. Rational Design of $Ti_3C_2T_x$ MXene Inks for Conductive, Transparent Films. *ACS Nano* **2023**, *17*, 3737–3749. [CrossRef]
126. Yuk, S.; Woo, S.; Kim, S.; Choi, S.; Byun, S.; Song, S.H.; Lee, D. Scalable Liquid-Crystalline MXene Films via Bio-Inspired Surface Bridging Strategy for Enhancing Electrochemical Performance. *Adv. Compos. Hybrid. Mater.* **2025**, *8*, 241. [CrossRef]
127. Awan, H.T.A.; Abdah, M.A.A.M.; Mehar, M.; Walvekar, R.; Chaudhary, V.; Khalid, M.; Khosla, A. MXene-Polymer Hybrid Composites for Advanced Energy Storage: Insights into Supercapacitors and Batteries. *J. Energy Storage* **2024**, *95*, 112449. [CrossRef]
128. Abdolhosseinzadeh, S.; Heier, J.; Zhang, C. Coating Porous MXene Films with Tunable Porosity for High-Performance Solid-State Supercapacitors. *ChemElectroChem* **2021**, *8*, 1911–1917. [CrossRef]
129. Dadashi Firouzjaei, M.; Nemani, S.K.; Sadrzadeh, M.; Wujcik, E.K.; Elliott, M.; Anasori, B. Life-Cycle Assessment of $Ti_3C_2T_x$MXene Synthesis. *Adv. Mater.* **2023**, *35*, 2300422. [CrossRef]
130. Zhang, T.; Shevchuk, K.; Wang, R.J.; Kim, H.; Hourani, J.; Gogotsi, Y. Delamination of Chlorine-Terminated MXene Produced Using Molten Salt Etching. *Chem. Mater.* **2024**, *36*, 1998–2006. [CrossRef]
131. Soundiraraju, B.; George, B.K. Two-Dimensional Titanium Nitride (Ti_2N) MXene: Synthesis, Characterization, and Potential Application as Surface-Enhanced Raman Scattering Substrate. *ACS Nano* **2017**, *11*, 8892–8900. [CrossRef]
132. Ungureanu, A.; Francini, A.; Neri, P.; Girimonte, A.; Giovanardi, R.; Ferrari, A.M.; Rosa, R. Systematic Life Cycle Environmental Impact Comparison of Alternative Synthetic Strategies for $Ti_3C_2T_x$ MXene. *ACS Sustain. Chem. Eng.* **2024**, *12*, 5893–5906. [CrossRef]
133. Kim, S.J.; Koh, H.-J.; Ren, C.E.; Kwon, O.; Maleski, K.; Cho, S.-Y.; Anasori, B.; Kim, C.-K.; Choi, Y.-K.; Kim, J.; et al. Metallic $Ti_3C_2T_x$ MXene Gas Sensors with Ultrahigh Signal-to-Noise Ratio. *ACS Nano* **2018**, *12*, 986–993. [CrossRef] [PubMed]
134. Kim, S.; Jo, H.; Yun, J.; Lee, J.-W.; Cho, J.; Kang, K.; Lim, H.-D. Sustainable and Eco-Friendly Syntheses of Green MXenes for Advanced Battery Applications. *Nano Converg.* **2025**, *12*, 39. [CrossRef]
135. Shuck, C.E.; Ventura-Martinez, K.; Goad, A.; Uzun, S.; Shekhirev, M.; Gogotsi, Y. Safe Synthesis of MAX and MXene: Guidelines to Reduce Risk During Synthesis. *ACS Chem. Health Saf.* **2021**, *28*, 326–338. [CrossRef]
136. Fang, H.; Thakur, A.; Zahmatkeshsaredorahi, A.; Fang, Z.; Rad, V.; Shamsabadi, A.A.; Pereyra, C.; Soroush, M.; Rappe, A.M.; Xu, X.G.; et al. Stabilizing $Ti_3C_2T_x$ MXene Flakes in Air by Removing Confined Water. *Proc. Natl. Acad. Sci. USA* **2024**, *121*, e2400084121. [CrossRef] [PubMed]
137. Habib, T.; Zhao, X.; Shah, S.A.; Chen, Y.; Sun, W.; An, H.; Lutkenhaus, J.L.; Radovic, M.; Green, M.J. Oxidation Stability of $Ti_3C_2T_x$ MXene Nanosheets in Solvents and Composite Films. *Npj 2D Mater. Appl.* **2019**, *3*, 8. [CrossRef]
138. Zhao, X.; Vashisth, A.; Prehn, E.; Sun, W.; Shah, S.A.; Habib, T.; Chen, Y.; Tan, Z.; Lutkenhaus, J.L.; Radovic, M.; et al. Antioxidants Unlock Shelf-Stable $Ti_3C_2T_x$ (MXene) Nanosheet Dispersions. *Matter* **2019**, *1*, 513–526. [CrossRef]

139. Liu, N.; Li, Q.; Wan, H.; Chang, L.; Wang, H.; Fang, J.; Ding, T.; Wen, Q.; Zhou, L.; Xiao, X. High-Temperature Stability in Air of Ti3C2Tx MXene-Based Composite with Extracted Bentonite. *Nat. Commun.* **2022**, *13*, 5551. [CrossRef]
140. Kamysbayev, V.; Filatov, A.S.; Hu, H.; Rui, X.; Lagunas, F.; Wang, D.; Klie, R.F.; Talapin, D.V. Covalent Surface Modifications and Superconductivity of Two-Dimensional Metal Carbide MXenes. *Science* **2020**, *369*, 979–983. [CrossRef]
141. Björk, J.; Rosen, J. Functionalizing MXenes by Tailoring Surface Terminations in Different Chemical Environments. *Chem. Mater.* **2021**, *33*, 9108–9118. [CrossRef]
142. Adomaviciute-Grabusove, S.; Popov, A.; Ramanavicius, S.; Sablinskas, V.; Shevchuk, K.; Gogotsi, O.; Baginskiy, I.; Gogotsi, Y.; Ramanavicius, A. Monitoring $Ti_3C_2T_x$ MXene Degradation Pathways Using Raman Spectroscopy. *ACS Nano* **2024**, *18*, 13184–13195. [CrossRef]
143. Choi, E.; Lee, J.; Kim, Y.-J.; Kim, H.; Kim, M.; Hong, J.; Kang, Y.C.; Koo, C.M.; Kim, D.W.; Kim, S.J. Enhanced Stability of Ti3C2Tx MXene Enabled by Continuous ZIF-8 Coating. *Carbon* **2022**, *191*, 593–599. [CrossRef]
144. Iqbal, A.; Hong, J.; Ko, T.Y.; Koo, C.M. Improving Oxidation Stability of 2D MXenes: Synthesis, Storage Media, and Conditions. *Nano Converg.* **2021**, *8*, 9. [CrossRef]
145. Zaed, M.A.; Tan, K.H.; Abdullah, N.; Saidur, R.; Pandey, A.K.; Saleque, A.M. Cost Analysis of MXene for Low-Cost Production, and Pinpointing of Its Economic Footprint. *Open Ceram.* **2024**, *17*, 100526. [CrossRef]
146. Lu, X.; Lian, G.J.; Parker, J.; Ge, R.; Sadan, M.K.; Smith, R.M.; Cumming, D. Effect of Carbon Blacks on Electrical Conduction and Conductive Binder Domain of Next-Generation Lithium-Ion Batteries. *J. Power Sources* **2024**, *592*, 233916. [CrossRef]
147. Jiang, M.; Jiang, D.; Cao, X.; Wang, J.; Sun, Y.; Zhang, M.; Liu, J. Scalable 2D/2D Assembly of Ultrathin MOF/MXene Sheets for Stretchable and Bendable Energy Storage Devices. *Adv. Funct. Mater.* **2024**, *34*, 2312692. [CrossRef]
148. Wan, S.; Li, X.; Chen, Y.; Liu, N.; Du, Y.; Dou, S.; Jiang, L.; Cheng, Q. High-Strength Scalable MXene Films through Bridging-Induced Densification. *Science* **2021**, *374*, 96–99. [CrossRef]
149. Rana, A.S.; Raza, N.; Anwar, M.J.; Nazar, M.F. Advancing MXenes through Green Chemistry for Sustainable Future. *Mater. Res. Bull.* **2025**, *193*, 113720. [CrossRef]
150. ECHA—REACH (EC No. 1907/2006). European Chemicals Agency. Available online: https://osha.europa.eu/en/legislation/directives/regulation-ec-no-1907-2006-of-the-european-parliament-and-of-the-council#:~:text=Search-,Regulation%20(EC)%20No%201907/2006%20%2D%20Registration%2C%20Evaluation,some%20on%2Dsite%20isolated%20intermediates (accessed on 23 August 2025).
151. Choi, J.; Oh, M.S.; Cho, A.; Ryu, J.; Kim, Y.-J.; Kang, H.; Cho, S.-Y.; Im, S.G.; Kim, S.J.; Jung, H.-T. Simple Approach to Enhance Long-Term Environmental Stability of MXene Using Initiated Chemical Vapor Deposition Surface Coating. *ACS Nano* **2023**, *17*, 10898–10905. [CrossRef]
152. Zhao, X.; Zhu, M.; Tang, C.; Quan, K.; Tong, Q.; Cao, H.; Jiang, J.; Yang, H.; Zhang, J. ZIF-8@MXene-Reinforced Flame-Retardant and Highly Conductive Polymer Composite Electrolyte for Dendrite-Free Lithium Metal Batteries. *J. Colloid Interface Sci.* **2022**, *620*, 478–485. [CrossRef]
153. Xu, H.; Liu, S.; Li, Z.; Ding, F.; Liu, J.; Wang, W.; Song, K.; Liu, T.; Hu, L. Synergistic Effect of $Ti_3C_2T_x$ MXene/PAN Nanofiber and LLZTO Particles on High-Performance PEO-Based Solid Electrolyte for Lithium Metal Battery. *J. Colloid Interface Sci.* **2024**, *668*, 634–645. [CrossRef]
154. Li, N.; Fan, J. Computational Insights into Modulating the Performance of MXene Based Electrode Materials for Rechargeable Batteries. *Nanotechnology* **2021**, *32*, 252001. [CrossRef]
155. Caffrey, N.M. Effect of Mixed Surface Terminations on the Structural and Electrochemical Properties of Two-Dimensional $Ti_3C_2T_2$ and V_2CT_2 MXenes Multilayers. *Nanoscale* **2018**, *10*, 13520–13530. [CrossRef]
156. Syamsai, R.; Rodriguez, J.R.; Pol, V.G.; Van Le, Q.; Batoo, K.M.; Adil, S.F.; Pandiaraj, S.; Muthumareeswaran, M.R.; Raslan, E.H.; Grace, A.N. Double Transition Metal MXene ($Ti_xTa_{4-x}C_3$) 2D Materials as Anodes for Li-Ion Batteries. *Sci. Rep.* **2021**, *11*, 688. [CrossRef]
157. Nykiel, K.; Strachan, A. High-Throughput Density Functional Theory Screening of Double Transition Metal MXene Precursors. *Sci. Data* **2023**, *10*, 827. [CrossRef] [PubMed]
158. Dihingia, K.D.; Saikia, S.; Yedukondalu, N.; Saha, S.; Sastry, G.N. 2D-Double Transition Metal MXenes for Spintronics Applications: Surface Functionalization Induced Ferromagnetic Half-Metallic Complexes. *J. Mater. Chem. C* **2022**, *10*, 17886–17898. [CrossRef]
159. Guan, Q.; Yan, H.; Cai, Y. Flatten the Li-Ion Activation in Perfectly Lattice-Matched MXene and 1T-MoS2 Heterostructures via Chemical Functionalization. *Adv. Mater. Interfaces* **2022**, *9*, 2101838. [CrossRef]
160. He, X.; Xiang, Y.; Yao, W.; Yan, F.; Zhang, Y.; Gerlach, D.; Pei, Y.; Rudolf, P.; Portale, G. MXene Surface Engineering Enabling High-Performance Solid-State Lithium Metal Batteries. *Adv. Funct. Mater.* **2025**, *35*, 2416040. [CrossRef]
161. Zhou, S.; Guan, Y.; Tan, L.; Li, X.; Zhu, H.; Zhang, Q.; Dong, Z.; Yang, N.; Cong, Y. Recent Advances in Multiple Transition Metal MXenes: Synthesis, Properties, and Applications in Energy Storage. *J. Energy Storage* **2025**, *120*, 116419. [CrossRef]

162. Li, N.; Zeng, Z.; Zhang, Y.; Chen, X.; Kong, Z.; Arramel; Li, Y.; Zhang, P.; Nguyen, B.-S. Double Transition Metal Carbides MXenes (D-MXenes) as Promising Electrocatalysts for Hydrogen Reduction Reaction: Ab Initio Calculations. *ACS Omega* **2021**, *6*, 23676–23682. [CrossRef]
163. Liu, M.; Hong, J.J.; Sebti, E.; Zhou, K.; Wang, S.; Feng, S.; Pennebaker, T.; Hui, Z.; Miao, Q.; Lu, E.; et al. Surface Molecular Engineering to Enable Processing of Sulfide Solid Electrolytes in Humid Ambient Air. *Nat. Commun.* **2025**, *16*, 213. [CrossRef] [PubMed]
164. Cao, C.; Carbone, M.R.; Komurcuoglu, C.; Shekhawat, J.S.; Sun, K.; Guo, H.; Liu, S.; Chen, K.; Bak, S.-M.; Du, Y.; et al. Atomic Insights into the Oxidative Degradation Mechanisms of Sulfide Solid Electrolytes. *arXiv* **2023**, arXiv:2310.00794. [CrossRef]
165. Gogotsi, Y. The Future of MXenes. *Chem. Mater.* **2023**, *35*, 8767–8770. [CrossRef]
166. Mim, M.; Habib, K.; Farabi, S.N.; Ali, S.A.; Zaed, M.A.; Younas, M.; Rahman, S. MXene: A Roadmap to Sustainable Energy Management, Synthesis Routes, Stabilization, and Economic Assessment. *ACS Omega* **2024**, *9*, 32350–32393. [CrossRef]
167. Roadmap to Commercialize All-Solid-State Batteries. In ACerS Bulletin/Ceramic Tech Today; Summarizing UCSD Roadmap Including Interface Stability, Process Scale-Up, and Recyclability Priorities. 2020. Available online: https://Ceramics.Org/Ceramic-Tech-Today/Roadmap-to-Commercialize-All-Solid-State-Batteries/?Utm_source=chatgpt.Com (accessed on 23 August 2025).
168. Zhao, Z.; Xu, Z.; Wang, Y.; Huang, W.; Cheng, Y.; Wong, W.-Y. Scalable Assembly of Flexible Ultrathin All-in-One MXene-Based Supercapacitors. *J. Mater. Chem. A* **2025**, *13*, 13175–13185. [CrossRef]
169. European Commission. *REACH Regulation (Regulation EC No. 1907/2006)—Overview and Legal Scope*; Updated 2025; European Chemicals Agency: Helsinki, Finland, 2006. Available online: https://Environment.Ec.Europa.Eu/Topics/Chemicals/REACH-Regulation_en (accessed on 23 August 2025).